Engineering 5 (2019) 954–969

Contents lists available at ScienceDirect

Engineering

journal homepage: www.elsevier.com/locate/eng

Research
Vehicle Engineering—Review

Thermal Management of Vehicle Cabins, External Surfaces, and Onboard Electronics: An Overview

Garrett J. Marshall [a], Colin P. Mahony [a], Matthew J. Rhodes [a], Steve R. Daniewicz [b], Nicholas Tsolas [c], Scott M. Thompson [c,*]

[a] Center for Advanced Vehicular Systems, Mississippi State University, Mississippi State, MS 39762, USA
[b] Department of Mechanical Engineering, The University of Alabama, Tuscaloosa, AL 35487, USA
[c] Department of Mechanical Engineering, Auburn University, Auburn, AL 36849, USA

ARTICLE INFO

Article history:
Received 2 November 2018
Revised 22 February 2019
Accepted 26 February 2019
Available online 1 June 2019

Keywords:
Vehicle design
Automotive engineering
Electronics packaging
Heat pipes
Climate control
Heating, ventilation, and air-conditioning
Battery cooling
Thermal soak

ABSTRACT

Reducing heat accumulation within vehicles and ensuring appropriate vehicular temperature levels can lead to enhanced vehicle fuel economy, range, reliability, longevity, passenger comfort, and safety. Advancements in vehicle thermal management remain key as new technologies, consumer demand, societal concerns, and government regulations emerge and evolve. This study summarizes several recent advances in vehicle thermal management technology and modeling, with a focus on three key areas: the cabin, electronics, and exterior components of vehicles. Cabin-related topics covered include methods for reducing thermal loads and improving heating, ventilation, and air-conditioning (HVAC) systems; and advancements in window glazing/tinting and vehicle surface treatments. For the thermal management of electronics, including batteries and insulated-gate bipolar transistors (IGBTs), active and passive cooling methods that employ heat pipes, heat sinks, jet impingement, forced convection, and phase-change materials are discussed. Finally, efforts to model and enhance the heat transfer of exterior vehicular components are reviewed while considering drag/friction forces and environmental effects. Despite advances in the field of vehicle thermal management, challenges still exist; this article provides a broad summary of the major issues, with recommendations for further study.

1. Introduction

Effective thermal management of vehicles requires new and enhanced systems and methods aimed at reducing the generation and displacement of heat within and around a vehicle. This can be accomplished either directly or indirectly, and can have significant impacts on a host of essential vehicle attributes, including fuel economy, safety, range, reliability, and overall comfort of the occupants. Most of these impacts impose secondary impacts; for example, improving a driver's comfort also tends to improve safety by enhancing alertness, and better component thermal management leads to enhanced electronic reliability. In the case of military applications, thermal management is also an essential factor in detection avoidance on the battlefield.

Numerous technological and engineering advancements have occurred over the last several decades to improve various facets of vehicle thermal management. This field has become increasingly important due to many motivating factors, including new vehicle features, consumer demand, societal concerns over fuel consumption and its political and environmental impacts, government regulations, reduced vehicle size, and the rise of electric, autonomous, and driverless vehicles.

This article serves as a survey and summary of recent research and engineering innovations related to vehicle thermal management methods and technologies. It is divided into three main sections, each focusing on one core area of vehicles in which thermal management plays an important role. The first section examines the cabin, which is a primary source of heat accumulation, especially during warm weather. This section looks at means of reducing heat ingress as well as improvements in climate control and ventilation systems, which have a substantial impact on fuel economy. The second section discusses the heat generation and cooling of electronic components; special attention is paid to electric vehicles, which experience unique thermal challenges not typically encountered in conventionally fueled vehicles. The third section

* Corresponding author.
E-mail address: smthompson@auburn.edu (S.M. Thompson).

https://doi.org/10.1016/j.eng.2019.02.009
2095-8099/

examines the thermal impacts of a variety of exterior vehicle components—including grills, brakes and tires, the exhaust system, and body aerodynamics—in addition to general weather and terrain considerations.

2. Cabin

The cabin consists of structural components that separate the internal, temperature-controlled environment from the external environment of a vehicle. In this regard, the cabin area serves as a main focal point in ensuring the overall comfort of the passenger, by not only providing an environment that allows for a pleasant driving experience, but also ensuring that the thermal conditions within the cabin are conducive to alert driving habits. Danca et al. [1] discuss the measurement and improvement of passenger comfort in detail.

A primary goal of cabin thermal management design is to minimize vehicle energy use while achieving a high level of passenger comfort. Vehicle heating, ventilation, and air-conditioning (HVAC) systems exert a large power demand on the vehicle's engine and battery, which can lead to reduced fuel economy. A study by Orofino et al. [2] involving a group of vehicles with different sizes and HVAC systems, and an average fuel economy of 41 US miles per gallon (MPG; 1 MPG $\approx 2.35\ \mathrm{L{\cdot}km^{-1}}$), demonstrated that fuel consumption increased by 23%–41% when the air conditioner (AC) was operating. Being able to reduce fuel consumption not only decreases gasoline cost for the vehicle owner, but also has a positive impact on the environment by reducing harmful emissions [3].

2.1. Heat load reduction

Over the last several decades, many technologies have been developed to keep passengers comfortable while decreasing the AC load and fuel consumption. These efforts have mainly focused on finding ways to reduce the amount of vehicular heat absorption—a phenomenon known as heat soak or thermal soak—when a vehicle is exposed to the sun for an extended period of time [3–13]. The methods explored have included cooling vehicle cabin zones independently [14–20], implementing automatic climate control (ACC) algorithms [21–29], managing air quality [7,28,30–32], and improving electric vehicle (EV) HVAC systems [33–37]. Each of these approaches is discussed below.

During thermal soak, a vehicle's cabin temperature increases until it reaches an equilibrium point. The amount of heat gained during the soak, and thus the equilibrium temperature, are influenced by the transmissivity the windows and windshield with respect to sunlight, the absorptive properties of the dashboard and interior components, and the temperature of the vehicle shell. In the winter or during colder months, thermal soaking is beneficial because it heats the vehicle's interior using available solar energy. However, during seasonally hotter months, thermal soaking results in heat that must be removed by AC or ventilation systems, thus greatly increasing ancillary loads. Researchers at the US National Renewable Energy Laboratory (NREL) have reported that reducing a Cadillac STS's thermal soak load by 30% during the summer months can reduce AC fuel use by up to 26% [4].

2.1.1. Glass shading

Glass shading refers to an entire class of technologies that involve altering glass in some way in order to decrease the effects of radiative heating. While vehicle glass shading is not a particularly new technology, different methods are still being developed to more effectively reduce heat gain while maintaining good visibility. One technology tested by the NREL in 2006 was Sungate® EP, a solar reflective glazing for vehicle glass surfaces. Two Cadillac STSs were heat soaked during the period between July and September, and thermal loads were recorded over a 24 h period for both an experimental and control vehicle [4]. Average air and seat temperatures in the experimental vehicle were reduced by 7.1 and 8.7 °C, respectively, while the windshield and dashboard temperatures were reduced by 19.3 and 14.6 °C, respectively [7]. Considering that solar radiation through glass is the largest contributor to a vehicle's thermal load [6], these significant temperature reductions can be attributed to the glazing, which transmitted only 33% of the total solar energy.

The NREL performed a subsequent test using a modified 2006 Toyota Prius, a plug-in hybrid electric vehicle (PHEV) with a 5 kW·h Hymotion lithium-ion energy storage system (ESS). After simulating and testing the vehicle on a dynamometer over multiple drive cycles, the researchers concluded that applying the reflective glazing to the front and rear windshields decreased the compressor power enough to improve fuel economy by 8% (going from 38.4 to 41.6 MPG) [8]. Ozeki et al. [9] performed a similar comparison of standard vehicle glass and an infrared (IR)-cut type glass, which has a higher solar reduction rate, on a medium-sized EV. Results from simulated summer conditions in a climate chamber showed that the heat load was reduced by 20% when the IR-cut type glass was used.

Glass surface glazings currently maintain a constant degree of transmissivity, but variable transmissivity would be preferable; that is, it would be better to have a higher transmissivity during cold weather to provide free passive solar heating to the cabin, and a lower transmissivity during hot weather to reduce thermal soak and cabin temperatures with minimal fuel-consumption penalty costs.

Electrochromic (EC) glazing is a technology that allows transmissivity to be controlled with an applied current. In 2003, Jaksic and Salahifar [10] determined that an EC glass windshield transmitted 2.5 times less solar power than a standard clear windshield. The results showed a decrease in the heat soak temperature inside the cabin, an increase in passenger comfort, and a reduced load on the HVAC system. Since an electric current is required to drive the change in transmissivity, a power source is necessary. One way of providing a power source is to connect the glass to the vehicle's battery. However, a more attractive method is to use photovoltachromic technology, in which the glazing harvests solar energy with a common dye-sensitized solar cell to power its color change. Cannavale et al. [11] created and tested the first working photovoltachromic device in 2014. The device responded to an increase of light intensity in less than 2 s and to a decrease of light intensity in less than 5 s, while allowing transmission of only 25% of radiation when exposed to 1.4 $\mathrm{kW{\cdot}m^{-2}}$ solar intensity. This result compares favorably with the 33% load reduction attained using Sungate® EP. Solar intensity was not quantified for this data, but data collection occurred while the vehicle was in direct sunlight.

2.1.2. Surface modifications

Researchers have also sought to reduce cabin temperature by lowering heat gain through the vehicle's skin [3,4,7,12,13]. In the NREL 2006 summer experiments to investigate heat soak temperatures, a solar reflective coating was tested against a control coating. The Cadillac STS (control group) was sprayed with a common basecoat, while a basecoat with IR-reflective pigments was used on a modified vehicle. Both cars were then sprayed with the same clear coat. When compared under a sun lamp, the panel surface with the reflective coating (0.82 absorptivity) was 9–10 °C cooler at equilibrium than the control panel surface (0.89 absorptivity) [4]. It is notable, however, that the percent reduction in panel temperature does not translate to an equivalent reduction of the air temperature in the cabin, due to roof insulation and various other existing heat transfer paths—especially through the windows. For example, in 2005, a less reflective coating was tested that decreased the roof exterior temperature by 6.7 °C compared with the baseline, but the cabin air temperature decreased by less than 1 °C overall. The modified vehicle in the 2005 experiment had a baseline gray paint with an absorptivity of 0.78 and a film-covered roof with an absorptivity of 0.55 [7].

As mentioned above, the difference in reflectivity between a reflective and non-reflective roof in the 2005 comparison was at most 0.23. Levinson et al. [3] demonstrated in 2011 that increasing overall solar reflectivity, ρ, by 0.50 can reduce the breath-level air temperature (i.e., the temperature of the air in the vehicle near what would be the driver's mouth) by 5–6 °C. To further assess the degree of reduction, two 2009 Honda Civic 4DR GX compact sedans, one black ($\rho = 0.05$) and one white ($\rho = 0.60$) were heat soaked in July 2010. The group used ADVISOR, a tool developed by the NREL, to estimate the fuel savings and emissions as a result of their experiment. The white car was estimated to require a 13% smaller AC unit than the black car to cool the cabin to 25 °C within 30 min. For a typical cool-colored shell ($\rho = 0.35$), assuming that AC capacity and engine ancillary load scale linearly with shell color, this capacity reduction resulted in an increased fuel economy of 0.24 MPG (1.1%). Major emissions were estimated to be reduced from 0.37% to 2.0% [3].

In the United States, long-haul trucks consume nearly 2×10^9 gal (1 gal ≈ 3.79 L) of fuel annually while idling, 8.38×10^8 gal of which are consumed during resting periods for passenger comfort in the sleeper cab [13]. Researchers from the NREL demonstrated that idling fuel consumption could be reduced by means of an insulation package. After adding insulation within the cabin walls and structural channels, the cooling load in the cabin was reduced by 34% and could be managed with a battery-driven, electric AC unit. It was noted that adding reflective paint to the cabin's exterior skin did not significantly contribute to thermal load reduction due to the vehicle's light color, although a darker vehicle might benefit more from such paint.

2.1.3. Ventilation

Properly ventilating a parked vehicle can decrease cabin temperature during thermal soak. In a test, the NREL incorporated an array of six solar-powered fans into the sunroof of a Cadillac STS. The results showed that pulling air out of the vehicle is more effective than pushing air in, and allows for a decrease in air temperature of 5–6 °C—approximately 26% of the maximum reduction possible [4].

In addition to venting the sunroof, the NREL performed tests on alternate ventilation configurations in a 2000 Jeep Grand Cherokee [7]. Some configurations included forced convection from instrument panel vents or sunroof fans, while others were passive and only required opening the sunroof and adding floor vents. The results from this study are shown in Fig. 1. Venting the floor increased natural convection significantly; however, the researchers noted that preventing exhaust products, dirt, and animals from entering the vehicle was problematic [7].

Saidur et al. [5] sought to improve the performance of a current solar-powered, parked-car ventilator [5]. The ventilator was mounted in the rear passenger windows of a metallic gray Nissan Sunny and was powered by the vehicle's battery and a roof-mounted 50 W solar panel. A larger motor and fan system was used to increase the ventilator's flow rate from 20 to 110.5 CFM ($ft^3 \cdot min^{-1}$; 1 CFM ≈ 0.028 $m^3 \cdot min^{-1}$), and data were collected between 11 a.m. and 4 p.m. Overall, the temperature was reduced by 11% compared with the unmodified ventilator. The solar panel provided 31.2 W to the ventilators on sunny days, with the remaining energy being used to charge the car battery. On overcast days, when the car battery was the sole power source, it was calculated that the ventilators could be operated for 7.2 h.

2.2. Zoned and individualized cooling

Zoned cooling is perhaps one of the most researched methods of reducing vehicular AC demand. It not only lets the vehicle occupants tailor the settings based on personal comfort requirements, but also allows better overall energy management of the HVAC system.

2.2.1. Zoned cooling

Cooling the greatest surface area in contact with a passenger—namely, the seat—permits better independent temperature control. Cooled seats ("seat conditioning") methods are not new, but the

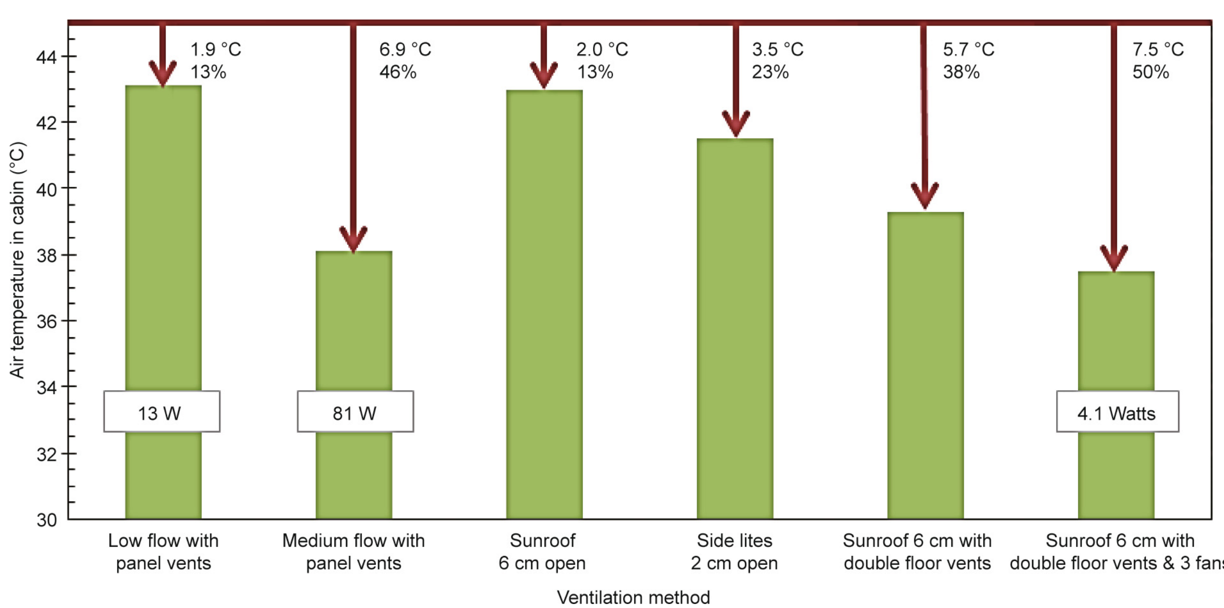

Fig. 1. Results of a ventilation technique study. The arrows represent the decrease in temperature compared to an unventilated, baseline cabin temperature (45 °C), while the ambient temperature is 30 °C. Bars labeled are those that require power, while those without labels are passive. Reproduced from Ref. [7] with permission of the National Renewable Energy Laboratory, © 2008.

technology is continually being optimized [14–17,38]. In 2007, one common method of seat climate control used fans embedded in the seat to push or pull cabin air cooled by a thermoelectric device toward or away from occupants. Rather than using unconditioned cabin air, engineers have designed augmented systems capable of passing conditioned air through ductwork linked directly to the seat ventilation system. Air can then be cooled or heated further by a Peltier element [14]. The Peltier effect can be thought of as a reverse Seebeck effect. In a Peltier device, electricity is used to create a temperature difference between two sides of the unit. An occupant can be heated or cooled by directed air from the hot or cold side of the module. Human tests with the augmented system demonstrated a reduced time-to-comfort of 4.5 min—2.5 min less than the time achieved using a thermoelectric device, and 1 min less than that using HVAC-air-cooled seats [14]. Another approach to seat conditioning is to use an asymmetric cooling scheme. Velivelli et al. [38] combined active cooling along the seat's lumbar support with ventilation-only in the seat cushion. Optimization of power to, and placement of, the cooling apparatus was carried out based on a human comfort-based model with predicted temperatures validated to within 1 °C of experiments.

Beyond seat conditioning, thermoelectric devices have recently been tested for use in counter-flow, air-to-air [39], and air-to-liquid [40] AC systems. Such systems can reduce engine load and may offer a less expensive, nonflammable solution to new Environmental Protection Agency (EPA)-regulated refrigerants. Though no testing has yet taken place within the context of a vehicle, simulations already exist that suggest methods of optimization for these thermoelectric AC systems [39,40].

To improve zoned cooling further, vents can be directed at different body parts of the cabin occupant, particularly the face, chest, and waist [15]. Tests were conducted to optimize the thermal comfort provided, and it was confirmed that this system cooled the cabin more effectively than a baseline whole-cabin cooling system. Participants were asked to rate their comfort level of different body parts during the baseline test (no spot cooling) while in the car cabin. The rating scale ranged from very uncomfortable (−4) to very comfortable (4) [15]. On average, the participants' body parts experienced an uncomfortable (−1) during the baseline, but when spot cooling was introduced and the participants were allowed to control their own temperature settings, average participant comfort rose to a comfortable 1.75–2 for all body parts. Participants also agreed that they were cooled quicker under transient conditions using spot cooling. In an effort to optimize the system, it was determined that cooling should use low flow rates to avoid dry eyes and to overcome "warm forehead" discomfort. Since the neck is a more sensitive area, some participants objected to neck or cheek cooling; however, low flow rates in these areas could be used during a thermal soak cooldown to more quickly improve transient comfort, and could then be turned off under steady-state conditions [15]. Simulations by Ghosh et al. [16] have shown that nozzles aimed at these areas cool occupants most effectively when paired with seat cooling.

In 2011, Kaushik et al. [17] simulated the thermal sensation and comfort produced by another localized/zonal cooling system. Their model was based on steady-state conditions and incorporated a human physiology model (based on the 50th percentile male) as well as a human thermal comfort model. Test data were collected from college students of different ages and genders who rated their comfort and sensation at a steady-state cabin temperature. Fig. 2 compares the predicted and measured results for several cooling methods [17]. In general, the results demonstrated that micro-cooling/heating strategies can provide sufficient thermal comfort at a potentially lower AC load based on the investigated steady-state temperature of 29 °C. A recent study by Ito et al. [41] characterized passenger comfort from similar secondary HVAC devices in various thermal scenarios. The research was conducted with actual vehicles in order to validate their heat balance model, which segmented a human body and considered a blood-flow-based heat transfer. The refined thermal comfort model provides a more effective means to design cabin/AC architectures and technologies for passenger comfort under various transient/non-uniform conditions.

The effects of zoned cooling on passenger comfort have been studied extensively; however, recent efforts have focused on quantifying its impact on the prime mover (e.g., the combustion engine and/or batteries). Wang et al. [18] used test data to design, test, and simulate a system that could readily be installed for commercial use in an existing vehicle. The battery-pack-powered system was placed in the trunk with the waste heat exchanger, control devices, and pumps. Power savings were based on steady-state environmental-tunnel test data taken from a Buick LaCrosse operating with standard and zoned cooling configurations. From the data, the researchers estimated a 29% power savings from the AC compressor. For greater power savings, sections of the zoned cooling system can be disabled when the vehicle is not fully occupied.

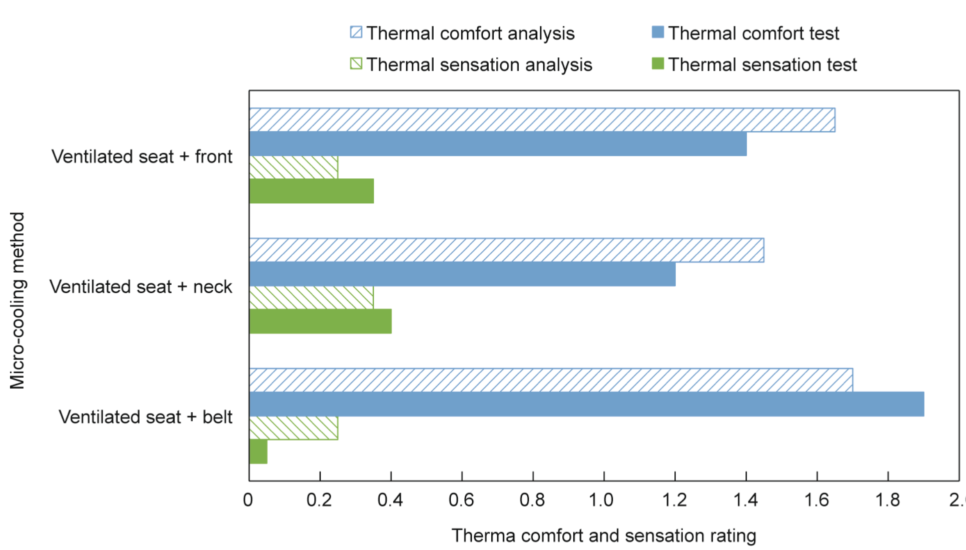

Fig. 2. Thermal comfort and sensation simulation compared with test results for three micro-cooling methods.

2.2.2. Individualized cooling

Cooling vehicle zones may manage the cabin environment effectively, but more individualized approaches are also possible and have the potential to complement onboard cabin-cooling methods. In 2010, Salaün et al. [19] investigated the incorporation of phase-change material (PCM) into clothing. By using microencapsulated PCM, they were able to store 163–170 $J\cdot g^{-1}$ of thermal energy after 13 thermal cycles. After each use, the PCM must be "recharged" by cooling the material back to a solid to complete a cycle and start anew. Although their development may be incorporated into textiles, certain phenomena caused the PCM capsules to wear out over time.

A simpler method of individual climate control was researched in 2013, when Massachusetts Institute of Technology (MIT) students developed a personalized cooling technology called "Wristify." The device uses the Peltier effect to cool a person's wrist at fixed time intervals. These changes in temperature occur at one-minute intervals and affect the thermal comfort of the entire body.

It should be noted, of course, that by nature, these solutions are not vehicle-specific. They are also not sufficient to completely eliminate HVAC systems. However, if used with in-vehicle methods, they could greatly reduce overall energy consumption [20].

2.3. Automatic climate control

ACC was first introduced in 1964 [21], and a similar derivative of the original analog linear controller is still widely used today. Wang et al. [22] improved upon the existing algorithm by separating transient and steady-state controls to make the path to steady state tunable/adjustable. An explicit accounting of passenger thermal inertia for thermal load estimations was also integrated into the model in order to reduce reliance on internal car temperature sensors. This new method allows a prototype vehicle to be calibrated within 4–6 weeks, and its graphical software package can be easily auto-coded and incorporated into an ACC microcontroller. The system was implemented in North American and Asia-Pacific vehicles over a three-year period and met or exceeded the standard system performance in terms of efficient and effective thermal control.

Fayazbakhsh and Bahrami [23] devised and simulated another type of AC model with the potential to optimize ACC. Their lumped system algorithm enables more efficient AC use by predicting and compensating for changes in thermal load when the algorithm is incorporated into a vehicle's computer with appropriate sensors. Using a similar method, Marcos et al. [24] developed and validated a thermal model and found that they could adequately calculate heat transfer into the cabin and estimate fuel consumption due to HVAC usage.

Donovan and Manning [25] performed a proof-of-concept ACC using a fuzzy-logic-based proportional integral (FPI) controller. Fuzzy logic is a type of programming logic that allows for "degrees of truth" rather than fixed values of "true" and "false." Its application allowed the model to be independent of a specific vehicle and limited the memory required for implementation. The system used carbon dioxide (CO_2) and IR thermographic sensors and an externally variable displacement compressor (for temperature and humidity management) in a multi-zone environment. Their scheme was able to control temperature and humidity in the zoned environment effectively and efficiently while maintaining safe CO_2 levels.

Another approach to ACC, in terms of classical control theory terminology, is to add a derivative term to the proportional integral (PI) controller in order to implement a proportional integral derivative (PID) controller, which is more precise than traditional ACC. Several industrial applications use the Chien–Hrones–Reswick (CHR) method to tune the PID gains [26]. Khayyam et al. [28] combined a PID controller with a neural network tuner (NNT) to reduce power consumption and increase the efficiency of a vehicle's HVAC system. This approach was not uncommon at the time, as Zheer-Uddin and Tudoroiu also tested a similar scheme. Khayyam et al., however, created a coordinated multi-control system (CMCS) that included a PID controller to control AC function and three stepper controllers to adjust recirculation gates and set points. The system monitored air temperature, humidity, and CO_2 concentration, and used these inputs to coordinate the evaporator (for temperature management), blower (for flow rate management), and ventilation gates (for CO_2 concentration management). Three simulations were performed using American Society of Heating, Refrigerating, and Air-Conditioning Engineers (ASHRAE) standards to set cabin comfort conditions, while Tokyo clear-day weather data and Federal Highway Driving Schedule (FHDS) data were used to model a real driving scenario. The first simulation used a manually tuned PID, the second was tuned using CHR, and the third used an NNT PID. The NNT demonstrated no overshoot, little instability, and a maximum energy reduction of approximately 14% for the given conditions [28].

A study conducted by Furse et al. [29] in 2014 gathered real-world data from a Hyundai Genesis climate-control system. Monitoring various parameters of American customer use via smart phones, they found that temperature and blower speed were controlled manually if the cabin temperature was under heat soak conditions at or above 35 °C (95 °F). However, under mild conditions, the ACC was used more often [29]. These findings suggest that ACC is improving and becoming more useful to customers.

2.4. EV air-conditioning systems

Ever-tightening emission standards have led to increased interest in EVs. An EV's limited driving range can be improved by implementing the aforementioned technologies and methods to reduce AC use, or by optimizing HVAC characteristics specifically tailored for EVs. HVAC systems for conventional internal combustion engines (ICEs) dispense some of their waste heat into the AC's condenser to enable an efficient air-conditioning cycle. As EV batteries do not reach the temperatures of ICEs, they cannot heat the condenser-side refrigerant adequately, and a different method must be used to heat and cool the vehicle.

The NREL has determined that maintaining cabin comfort in cooling situations reduces EV range by 35%–50% [33]. Simulations performed by Kambly and Bradley [34] using weather data for the United States throughout the year showed that even more energy is consumed to heat the cabin of a PHEV. Torregrosa-Jaime et al. [35] noted that the challenge of cabin heating also exists in fully electric vehicles (FEV). An EV conventionally relies on electric heaters and coolers. However, despite the necessity of using electricity to run a compressor, one way to move toward a more efficient system involves the incorporation of heat pumps.

Greater research focus has been given to implementing heat pumps in electric buses than in cars. Torregrosa-Jaime et al. [35] developed a dynamic modular model to calculate the energy consumed by a heat pump and auxiliaries (cabin blowers, circulation pumps, and radiator fans) in an electric bus. The tool was validated using a conventional vapor compression heat pump, as used on a Daily Electric minibus, but the tool can be adjusted to calculate energy consumption for any EV. This model would help size components and optimize control strategies in mobile AC systems. The researchers' analysis revealed that blowers and fans consumed a significant amount of energy (29%–40% of the total) and could be optimized to lower energy consumption depending on the vehicle and operating conditions. Nielsen et al.'s [42] simulated energy consumption from the blower is in agreement with these values.

Cho et al. [36] designed an experiment to study the performance of heat pumps using waste heat from the electronics associated with an electric bus. A controllable test setup using R-134a refrigerant was constructed to mimic the systems typically used to heat an electric bus. It was found that increasing the evaporator volumetric flow rate and increasing the outdoor temperature decreased the coefficient of performance (COP). However, the COP increased with increased condenser flow rate. A COP of 3.0 and a heating capacity of 30.0 kW was achieved when the system ran at an outdoor temperature of 0 °C with 0.020 and 0.040 $m^3{\cdot}min^{-1}$ flow rates through the condenser and evaporator sides, respectively. The chiller was set to pump water into the evaporator at 15 °C to approximate the amount of heat output from the bus electronics. Air temperature at the heater cores was measured and reached a maximum of 45 °C after 15 min. To increase thermal response and raise the temperature to the 50 °C minimum achieved by ICEs, it was suggested that a positive temperature coefficient (PTC) heater be added to the system [36].

In an effort to remove the dependence of cabin heating on battery power completely, Taylor et al. [37] designed and tested a thermal battery that heated an EV in a 10 °C ambient environment for 1 h. They designed the thermal battery module and cooling loop for the system, and tested the output without system integration into a vehicle. The thermal battery used the PCM erythritol, a sugar alcohol, to store thermal energy for eventual transfer to the working fluid (i.e., water) flowing through coiled copper tubing in an insulated PCM container. This design was portable, weighed 20 kg, and was roughly half the cost of the conventional lithium-ion battery used to power the heater. Although the thermal and lithium-ion battery capacity and specific power density were comparable, the thermal battery was physically larger and had a shorter shelf life. The researchers also noted that thermal management of the battery could reduce EV efficiency greatly [37], as discussed by Vlahinos and Pesaran [43].

3. Electronics

Before EV and hybrid electric vehicle (HEV) engines can perform comparably to ICEs, the high heat fluxes associated with the battery pack operation and insulated-gate bipolar transistors (IGBTs) must be effectively managed. In an HEV, direct current (DC) supplied to the motor by the battery pack must first be inverted to alternating current. A significant component of the inverter, the IGBT, transmits a large amount of energy during the process and must be thermally managed to maintain safe operation. The thermal conductivity of IGBT substrates will affect thermal management efficiency, but have been excluded from this review due to a lack of information in the literature. Current battery packs can also experience reduced lifetimes and must be thermally managed to promote longevity.

3.1. Passive IGBT cooling

Heat pipes are a relatively mature technology, having been first introduced around 1960 [44]. Noted primarily for their ultra-high thermal conductivity, a heat pipe is a passive heat transfer device that consists of a container with an internal fluid and/or wicking structure [44–46]. One type of heat pipe is the oscillating (or pulsating) heat pipe (OHP or PHP). The OHP is a two-phase, wickless device with serpentine-arranged tubes filled partially with a working fluid. When a temperature difference is imposed at opposite ends of the OHP, vapor bubbles and liquid slugs form in the evaporator (heat reception) and condenser (heat rejection) regions, respectively. The continuous oscillation and constant phase change of the working fluid drives increased heat transfer through the device. Recent advancements in OHP technology have been reviewed [46] and factors such as fill ratio, heat pipe geometry, and inclination angle have been shown to affect heat transfer. Fig. 3 illustrates the general anatomy of an OHP.

The harsh vehicular environment—which includes accelerations, inclinations, rapid air movement, and so forth—can affect the performance of heat pipes, and must be considered in automotive applications. Such factors have been studied experimentally by Burban et al. [47] with the use of a closed-end (open looped) OHP for a hybrid vehicle's IGBT. The performance of the OHP was tested using varying air temperatures (10–60 °C), air velocities (0.25–2 $m{\cdot}s^{-1}$), inclination angles (45°, 0°, and −45°), and working fluids (acetone, methanol, water, *n*-pentane, and R-134a). The testing incorporated six cartridge heaters inserted into a 120 mm × 80 mm copper plate to simulate a vehicle IGBT. The heat pipe was charged to a fill ratio of 50% and tested with input power levels ranging from 25 to 550 W. The researchers concluded that OHP thermal performance improves with increasing heat inputs. In general, thermal resistance decreased with increasing air temperature and velocity, with the exception of tests with acetone and *n*-pentane. Inclinations where the evaporator was above the condenser (−45°) resulted in unfavorable thermal performance, while the +45° position proved to be only slightly more favorable in general than the horizontal inclination. It was also found that R-134a did not serve well as an OHP working fluid under these conditions, as it was outperformed significantly by the other fluids tested. Acetone and *n*-pentane exhibited especially desirable results at lower power levels and air temperatures, while the thermal performance of water and methanol increased gradually as air temperature and input power increased.

The use of similar cooling technologies for military electronic devices was examined by Connors and Zunner [48]. Four methods of conducting heat to a liquid-cooled edge were modeled and tested: a heat pipe, a vapor chamber, a 6061-T6 aluminum plate, and a C00110 copper plate. Both the heat pipe and vapor chamber were made from copper with sintered wicks and used water as the working fluid. Three central heating blocks produced varying CPU-type power, while two outer blocks output a constant 40 W to emulate auxiliary components such as graphics processors. Two liquid-cooled rails at 74 °C were used to remove heat from the device. The researchers found that the vapor chamber, followed by the heat pipe, outperformed the copper and aluminum plates. By testing varying device orientations, they also determined that the thermal resistance of the vapor chamber and heat pipe was not dependent on gravity for the power level tested. It was also noted that the vapor chamber tested was more than twice as heavy as the heat pipe.

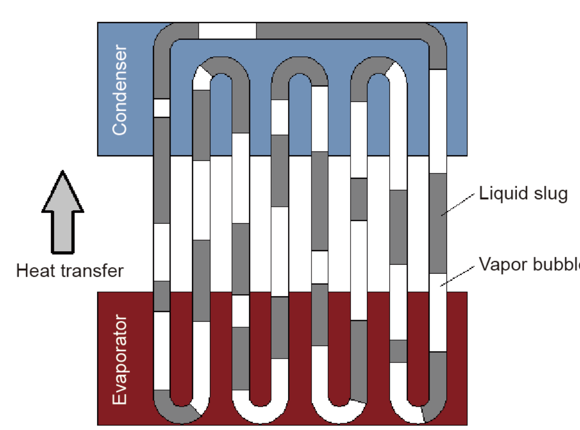

Fig. 3. OHP operation with evaporator, condenser, liquid slugs, and vapor bubbles illustrated.

Tang and Park [49] examined the use of a novel capillary two-phase loop (CTPL) device that can withstand the high vibrations found in vehicular applications. With traditional loop heat pipes (LHPs), the capillary evaporator transfers heat to the working fluid, creating a meniscus at the liquid/vapor interface that moves the working fluid from the condenser to the reservoir via capillary action. Vibrations can destroy the meniscus and impede fluid flow within the LHP. To diminish the effects of these vibrations, Tang and Park considered a CTPL that uses an evaporator with a primary fine wick that creates strong capillary forces to counteract vibrations more effectively. The primary wick is surrounded by a more porous secondary wick that can quickly supply liquid from the reservoir to the evaporator. The CTPL was tested under stationary and shock-induced conditions. Results from the vibration tests were comparable to the stationary results.

3.2. Thermal interface materials

Thermal interface materials (TIMs) have been used in the electronics industry for decades for applications such as improving heat transfer between computer CPUs and heat sinks. Otiaba et al. [50] assessed the use of TIMs for automotive electronics—more specifically, for the engine control module (ECM). The surface roughness of both the printed circuit board (PCB) and heat sink create small air gaps between the two surfaces that increase thermal resistance. The use of a TIM between the two surfaces can improve heat transfer significantly. In addition to having high thermal conductivity, TIMs are expected to be robust with respect to environmental and ambient conditions, reduce thermal stress between two regions with very different coefficients of thermal expansion, have low viscosity at operating temperature, have a long working life without leakage, and have the ability to deform easily over both mated surfaces with a relatively small thickness. Otiaba et al. [50] listed (and subsequently investigated) six types of TIMs, including: thermal grease, thermal pads, PCMs, gels, thermal conductive adhesives, and solders. Fig. 4 illustrates the application of a TIM to a generic electronics component and heat sink. Note that ensuring direct contact between the electronics and coolant can effectively remove the contact resistance [51]. The characteristics of TIMs have been improved in recent years through the addition of carbon nanotubes in the materials, which enhances the flexibility and thermal transport properties. These TIM enhancement methods have not been included in the present review because they have not yet been implemented within common electric/hybrid vehicle components. Examples of updated TIMs may be found in Refs. [52–55].

3.3. Active IGBT cooling

Vetrovec [56] studied the thermal performance of a novel active heat sink (AHS) design to cool the electronics on HEVs and PHEVs alike. The AHS was designed to replace the traditional cooling layout of an HEV's IGBT. In essence, an AHS is a sealed miniature loop of liquid metal alloy, such as galinstan. Forced convection from the electromagnetically controlled galinstan loop transfers heat from the electronics directly to the existing coolant loop or ambient air. Using finite element analysis (FEA), the thermal characteristics of the AHS design were studied under expected environments. The AHS successfully maintained an IGBT (operating at 244 W) at an acceptable operating temperature of 125 °C using an engine coolant loop at 105 °C. The simulation yielded a thermal resistance of 0.08 $°C·W^{-1}$. Another simulation of the engine coolant running anti-parallel to the galinstan loop exhibited similar results. The AHS was also modeled with ambient air at 50 °C, without engine coolant, and was shown to be capable of maintaining the IGBT operating temperature with a thermal resistance of 0.30 $°C·W^{-1}$.

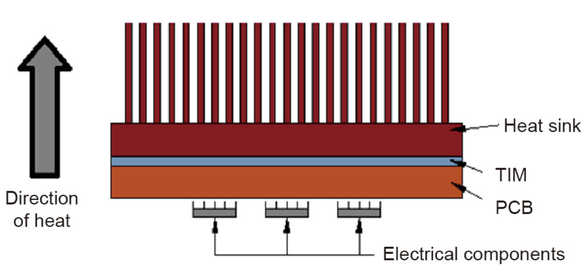

Fig. 4. Cross-section showing the use of TIM in a heat exchanger to transfer increased amounts of heat from the PCB to the heat sink. Reproduced from Ref. [50] with permission of Elsevier Ltd., ©2011.

Woo et al. [57] investigated the improvement of active water cooling for an IGBT inside an HEV inverter. Using an inverter with an integrated metal pipe and water at 60 °C, different pipe configurations were simulated with a 1.8 kW IGBT heat source in order to identify the optimal design (Fig. 5). Out of the five tested configurations shown in the figure, Configuration (iv) initially yielded the best performance. After further improvement, however, Configuration (vi) ultimately gave the best performance, with the lowest maximum surface temperature of 78.4 °C with an extra horizontal cross-pipe.

Other types of active cooling, such as spray and jet impingement, have also generated interest. Mudawar et al. [58] investigated the viability of integrating spray cooling for electronics onboard HEVs. A proposed implementation solution is shown in Fig. 6(a). The vehicle AC loop was modified by adding a pump and integrating a spray chamber for the electronics. This configuration required both the AC and electronics working fluids to be the same, typically R-134a. As shown in Fig. 6(b), a second configuration used an additional dedicated loop to cool the electronics. The working fluid for this loop is independent of other loops, but could add a significant amount of weight to the vehicle. Different working fluids were analyzed, and the liquid coolants R-134a and—even more so—HFE-7100 were found to be the most effective. HFE-7100 was predicted to maintain a surface temperature of 125 °C with a heat flux of 200 $W·cm^{-2}$. Experimental data were collected to successfully validate the simulation.

Two-phase spray cooling of the underside of automotive power inverters was investigated by Fluxes et al. [59]. As shown in Fig. 7, the study involved two pressure-atomized nozzles that sprayed antifreeze coolant at 88 °C on the bottom of thick-film resistors to simulate the IGBT for an HEV inverter. The spray array was tested and compared against a commercially available heat sink for heat fluxes up to 400 $W·cm^{-2}$. The spray array successfully removed 350 $W·cm^{-2}$, while maintaining the simulated IGBT at a maximum operating temperature of 125 °C. In contrast, the commercial heat sink removed only 64 $W·cm^{-2}$ at the same operating temperature. The reliability of the spray cooling was also assessed by over 2000 h of testing. Consistent thermal performance was observed throughout the test, demonstrating that the cooling method is robust and reliable.

Nucleate boiling occurs when the surface temperature is higher than the saturation temperature of the impinging fluid. The surface is said to be at a critical heat flux when the boiling rate is balanced by the liquid supply. This decreases the wetting surface, and a dry-out phase ensues. Fig. 8 illustrates the critical, or maximum, heat flux.

Narumanchi et al. [60,61] studied the implementation of nucleate boiling impinging jets and single-phase self-oscillating jets on power electronics such as IGBTs. The nucleate boiling impinging jet was modeled and compared with experimental data from the open literature, with good agreement. It was observed that there

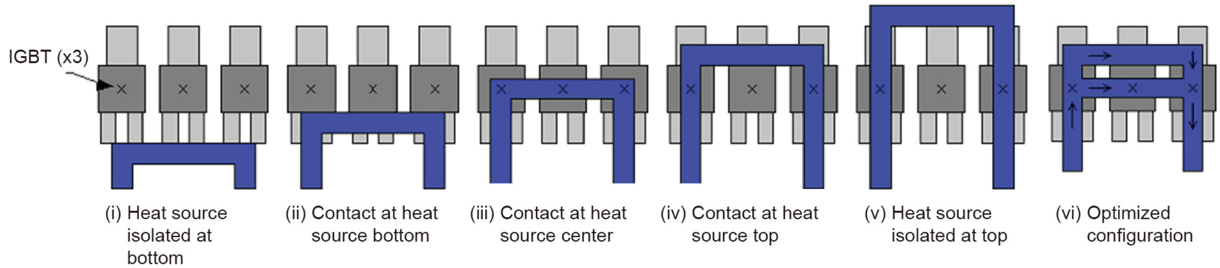

Fig. 5. (i–v) Initial simulated cooling pipe configurations to control IGBT temperature; (vi) optimized cooling pipe configuration based on the previously simulated configurations of (i–v). Reproduced from Ref. [57] with permission of IEEE, ©2009.

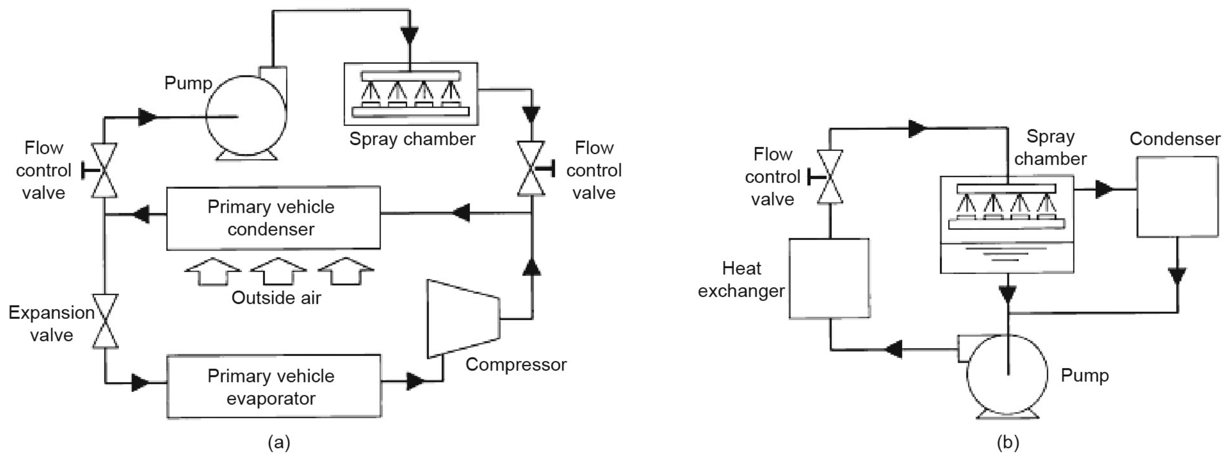

Fig. 6. Cooling of hybrid vehicle power electronics by (a) modifying the existing R-134a air-conditioning refrigeration loop and (b) using a separate cooling loop with an appropriate coolant. Reproduced from Ref. [58] with permission of IEEE, ©2009.

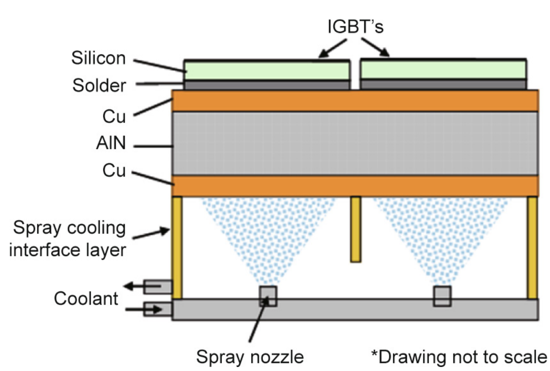

Fig. 7. Schematic of a pressure-atomized, spray-cooled power inverter module. The spray array successfully removed 350 $W\cdot cm^{-2}$, while maintaining the simulated IGBT at a maximum operating temperature of 125 °C. Reproduced from Ref. [57] with permission of IEEE, ©2012.

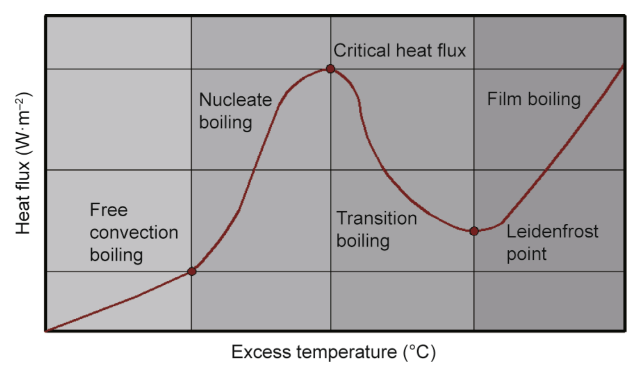

Fig. 8. General boiling curve for saturated liquids.

may be some benefit in using boiling jets on an IGBT, although some heat flux and jet velocity combinations may not yield significant improvement.

A single-phase, self-oscillating jet is a passive device that uses the interior geometry of a nozzle to create interacting fluid vortices that lead to subsequent oscillations in the fluid downstream from the nozzle. Narumanchi et al. [60,61] experimentally evaluated several designs of these oscillating jets under free and submerged configurations, as well as varying target distances and flow rates. The results were compared against a steady jet. No heat transfer benefits were found in the submerged configuration; however, in a free-surface configuration, this specialized jet outperformed steady jets by up to 30%. The oscillating jet also sustained a more uniform temperature distribution across the target surface.

3.4. Battery cooling

The performance of EVs and HEVs is highly dependent upon the battery pack. Since these components produce (when discharging) and receive (when charging) large amounts of electrical energy, which is accompanied by waste heat generation, thermal management considerations are critical to prevent overheating. During overcharge, a lithium-ion battery can reach internal temperatures of up to 200 °C and surface temperatures of up to 100 °C. These surface values can vary considerably with changes in operating or boundary conditions [62]. Furthermore, non-uniform temperature distributions within the battery can lead to localized deterioration and reduce the overall lifespan of the battery. Several battery-cooling methods have been studied in the past, including forced convection, PCMs, and heat pipes [63]. A comprehensive review of battery-cooling methods has been provided by Wang et al. [64], who described general considerations in choosing lithium-ion batteries and provided an analysis of their thermal management practices.

Swanepoel [65] proposed the implementation of an OHP to cool HEV batteries. As shown in Fig. 9 [63], lining the battery packs with OHPs facilitates heat transfer to the sides of the vehicle, allowing forced air convection to remove heat from the batteries while the vehicle is in motion. It was found that the battery–OHP contact resistance accounted for 65% of the total thermal resistance of the system. To reduce this large contact resistance, it was suggested that OHPs could be manufactured directly into the battery wall material.

Rao et al. [66] studied battery thermal management with a series of heat pipes. Four heat pipes charged with water at a fill ratio of 50% ± 5% were used to transfer heat from an aluminum heating block to a water module. The heating block simulated the power and area of a $LiFePO_4$ battery, and the maximum temperature could be maintained below 50 °C with less than 50 W of heat transfer. Furthermore, the heat generation did not surpass 30 W at the optimal temperature difference. Following the heat pipe experiment, Rao et al. [67] replaced the series of heat pipes with an OHP. These tests revealed additional benefits when the hotter side of the battery was positioned closest to the water bath condenser region. The OHP was also tested horizontally, but this configuration allowed the working fluid to flow back into the condenser, which accumulated fluid and created an undesirable drying effect. Greco et al. [68] compared the thermal performance of lithium-ion batteries cooled by heat pipes and forced convection. Simulations predicted that a heat pipe with free convection would reach a maximum temperature of 27.6 °C, while the battery under forced convection would reach a maximum temperature of 51.5 °C.

Combining heat pipes with forced convection, Tran et al. [69] examined a lithium-ion battery under typical vehicular operating conditions. Charged with demineralized water, the heat pipe's wick geometry featured a helical groove that spiraled along the length of the device. The evaporator region was placed in contact with the battery, while the condenser region was angled upward to separate it from the battery and reach more ambient air (Fig. 10) [70]. Finned plates were placed on the condenser section to increase the surface area and improve thermal performance. As shown in Fig. 11, the heat pipe and finned plate comprised a cooling module. Four heat pipes were placed around the battery module and tested at inclinations of −20°, 0°, and 20° from the vertical.

The results showed that the inclination angle had a minimal effect on the cooling performance of the heat pipe module, indicating that the heat pipe performance is nearly independent of gravity during reasonable vehicular conditions. However, gravity may help to increase heat transfer performance when paired with a heat pump air-conditioning system while the battery is in a preheating mode [71]. The results from Tran et al. also demonstrated that the cooling module benefited greatly from forced convection of any

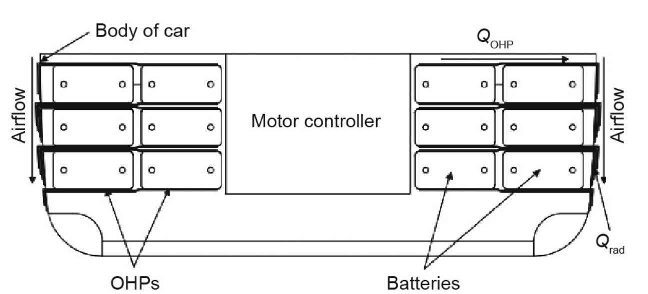

Fig. 9. Schematic of OHPs transferring heat away from batteries into the ambient air around a vehicle. Q_{OHP}: heat transfer of OHPs; Q_{rad}: radiation heat transfer. Reproduced from Ref. [63] with permission of Elsevier Ltd., ©2011.

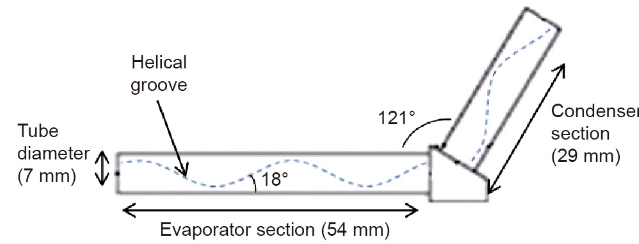

Fig. 10. Schematic of heat pipe with helical groove used in the experimental setup of Tran et al. Reproduced from Ref. [70] with permission of Elsevier Ltd., © 2014.

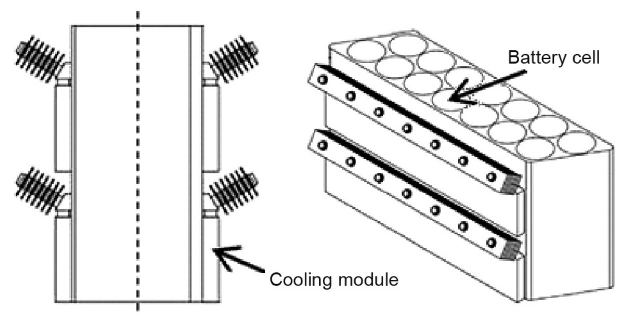

Fig. 11. Battery-cooling system assembly. The heat pipe and thin plate comprise the cooling module, which was tested at angles of −20°, 0°, and 20° from the vertical. Reproduced from Ref. [70] with permission of Elsevier Ltd., © 2014.

magnitude, and that the difference between free convection and relatively low ventilation is significant. In the context of vehicles, heat pipes must not only meet specifications to maintain the operating temperature of the battery, but also do so efficiently in a confined space. In a similar study, Tran et al. [70] tested flat heat pipes and heat sinks on a battery module. The results showed that the flat heat pipe reduced the system's thermal resistance by 30% in free convection and 20% in low air velocities when compared with a heat sink alone. The heat pipes also maintained efficiency in vertical and horizontal orientations, further confirming that this device can be used for thermal management during on-road conditions.

Thermal management using PCMs has also attracted interest over the last decade. PCMs store and release latent heat when the material changes phase (usually from solid to liquid, and vice versa). These materials can be useful in vehicle applications because they are relatively light and compact, and are highly efficient. A variety of chemical substances may be chosen as PCMs, based on thermal properties such as latent heat and melting point. A common problem with PCMs is their low thermal conductivity (about 0.10 $W \cdot m^{-1} \cdot K^{-1}$). Thermal enhancers such as metal foams have been incorporated into PCMs to improve their performance in this area. PCM thermal management techniques have shown great potential in their ability to maintain the temperatures of electronics, but these systems are only appropriate for periodic use. There is a point at which PCMs reach latent heat capacity and can no longer extract heat through phase change. If electronics impose heat fluxes while the PCM is at capacity, the heat will be conducted through the material at its poorest thermal conductivity [72].

Ling et al. [73] examined the use of PCMs on power batteries in order to determine the best material for this application. Paraffin/expanded graphite (EG) composites were applied to a battery and simulated to verify experimental results, which suggested that the best temperature range is 40–45 °C. These high-density paraffin/EG composites demonstrated an increased thermal conductivity (5–11 $W \cdot m^{-1} \cdot K^{-1}$) and high latent heat when compared with other

PCMs. It was found that PCMs with a low paraffin mass fraction exhibited low specific enthalpy but a higher thermal conductivity. The study concluded that a 75% paraffin mass fraction was optimal for the battery-cooling application. Studying the effects of PCM thermophysical properties is essential to improving the design of PCM devices.

4. Exterior

Overall vehicle performance and thermal management are both affected by external factors such as air flow through the grill, use of the brakes and tires, and heat generated in the underbody. Issues related to terrain and weather (aside from solar heating) should also be carefully measured and modeled when simulating a vehicle for thermal management assessment.

4.1. Front grills

In addition to aesthetics, the design of the front grill of the vehicle is important for thermal management because it controls the amount of cool air flowing through the radiator into the engine compartment. In addition, the front grill opening, condenser, and radiator contribute significantly to the total aerodynamic drag on the vehicle.

Xu et al. [74] demonstrated that a smaller grill area and larger cooling fan can reduce aerodynamic drag in a midsize sedan. They simulated a vehicle with three grill opening areas (197, 498, and 809 cm^2) and three fan power levels (270, 480, and 720 W) using experimental data obtained from wind tunnel and dynamometer tests. The results correlated the grill area and fan power in terms of fuel economy, which is useful in matching the grill opening to the fan power for optimal fuel efficiency [74]. Jama et al. [75] similarly studied the impact of grill area on aerodynamic drag by testing four grill configurations and varying the amount of air allowed through. Out of the four configurations, vertical strips along the grill were found to adequately shield cooling intakes while both minimizing drag (7% reduction) and allowing proper cooling flow to the radiator. The reduced drag was predicted to reduce fuel economy by about 1.7%.

Varying the opening of the grill was likewise employed by Charnesky et al. [76], who determined that restricting flow through the engine compartment can reduce aerodynamic drag only when cooling requirements through the condenser and radiator are minimal. An example of an active grill shutter (AGS) system was proposed by Pfeifer [77]. These systems can reduce engine warm-up time (which is when the greatest amount of emissions occur) when closed, but also allow sufficient cooling flow when needed. According to Pfeifer, the (EV) Tesla S incorporated AGS, which increased the distance the vehicle could travel while cooling the battery system. As these systems improve, active shutters must be optimized with the fan to provide optimum air flow to the air cooler and radiator heat exchangers. Such a synchronization may benefit from model predictive control, as shutter actuation can have a nonlinear influence on overall system cooling [78].

Kubokura et al. [79] studied different methods to reduce aerodynamic drag without adding new shutter components to the condenser, radiator, and fan module; instead, they investigated modifications in the external flow, fan control, and fan shrouds. For external flow modifications, they proposed moving the open area of the grill to a lower pressure section on the vehicle front in order to change the pressure balance and reduce aerodynamic drag. The researchers demonstrated this idea with the addition of a deflector to control air flow (Fig. 12). Air flow was also manipulated by turning off or reversing the direction of the fan. Although both scenarios experienced reduced drag, fan reversal was determined to be the better solution. The fan was also moved closer to the radiator, with a hole placed in the shroud directly behind the bumper reinforcement. In this configuration, air flowed without creating vortices/interference [80] (Fig. 13).

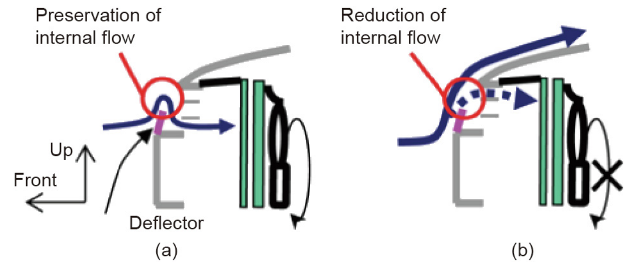

Fig. 12. Schematic of the side of a vehicle with the deflector at (a) low speed (cooling fan on) and (b) high speed (cooling fan off). The deflector is used to move the grill opening from an area of high pressure to one of lower pressure. Reproduced from Ref. [79] with permission of SAE International, © 2014. Further distribution of this material is not permitted without prior permission from SAE International.

Baeder et al. [80] has defined "interference" as the interaction between cooling air and external aerodynamics, and has identified it as the principle contributor to overall aerodynamic drag. They sought to prove that directed cooling air flow in the grill and engine compartment could reduce aerodynamic drag on the vehicle while increasing pressure at the grill. At the opening of the grill, a high-pressure area forms while the vehicle is in motion, while a low-pressure area occurs at the rear of the vehicle. Baeder et al. showed that the tail geometry of a vehicle affected the pressure drop with two different designs: an SAE bluff body and a scaled real body. Experimental data were obtained in wind tunnel tests on different SAE body configurations and agreed well with the computational results. For the computational fluid dynamics (CFD) simulations, four tail end designs were implemented along with three duct angles (90°, 45°, and 0°) to direct cooling flow within the engine compartment. The radiator was simulated with a "honeycomb" design using five levels of flow resistance. The analytical portion of the research was formulated using potential theory. Baeder et al. concluded that the experimental, simulation, and potential theory results were consistent, and that the interference effects could be concentrated in certain directions in the engine compartment in order to reduce the pressure in all high-pressure areas except the grill inlet.

Kuthada and Wiedemann [81] investigated the causes of cooling air drag on a vehicle using numerical and experimental efforts. As expected, most of the drag occurred at the front of the vehicle where air flow is sharply redirected by the hood. Front wheel com-

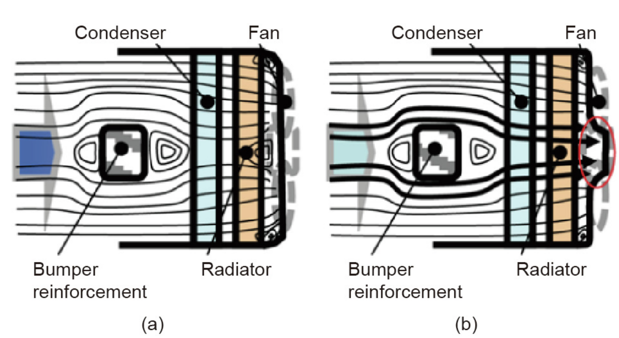

Fig. 13. Side view of the condenser, fan, and radiator configurations with air flow from the grill of the vehicle. (a) Original; (b) modified shape. A hole in the fan shroud allows air to flow without forming vortices in the modified shape. Reproduced from Ref. [79] with permission of SAE International, © 2014. Further distribution of this material is not permitted without prior permission from SAE International.

partments were also found to create significant drag after receiving redirected air from the engine compartment. Other areas and components, such as the firewall, axle, and exhaust system, contribute to drag forces as well, although to a lesser extent. These researchers also simulated vehicles with two rear-end geometries—notch-back and square-back—and found that the notch-back rear-end had a larger cooling air drag compared with the square-back.

4.2. Brakes

As weight constraints evolve to improve vehicle fuel economy, brake systems should evolve in tandem, in order to ensure stable contact friction for smooth stopping and to permit better convective heat transfer capabilities. In a typical vehicular wheel design, the rotor is the primary component of the brake system to reduce vehicular motion or hold it stationary. Upon application of the brake pedal, brake fluid is pumped to actuate the brake calipers in order to squeeze a pair of pads against the rotor. This causes an increase in friction; hence, heat is generated and the rotational speed of the wheel reduces. During braking, the heat induced by this friction can cause the rotor to experience temperatures ranging from 300 to 800 °C [82], resulting in an extreme thermal environment that can distort and degrade the brake materials. In fact, during emergency braking scenarios, temperature fields can be highly localized, with sharp gradients in the axial and radial directions [83]. To avoid such excessive temperatures, rotors with high thermal conductivity, specific heat, and density should be used [84].

Belhocine and Mostefa [82] conducted a coupled finite element thermal and stress analysis on gray cast iron rotors (FG25AL, FG20, and FG15) and corresponding brake pads. Two different styles of rotors were simulated: a solid body design and a ventilated rotor consisting of two disks with separating blades for air flow (Fig. 14) [85]. The results indicated that rotor ventilation plays a significant role in managing rotor temperatures. Munisamy et al. [85] proposed that changing the angle of the blades would increase the amount of cooling air flow, and therefore enhance heat transfer. Using both CFD and experimental methods, the blade angle were varied from 0° to 45° with boundary temperatures of 100 and 25 °C for the rotor and environment, respectively, while fin thickness was kept constant. Experimental and CFD results demonstrated that air flow was greatest with the 45° configuration, and recirculation was completely eliminated at 30°. Under extreme driving conditions, such as those experienced in racing, a curved-blade rotor design may even be worth considering for further heat dissipation enhancement [86].

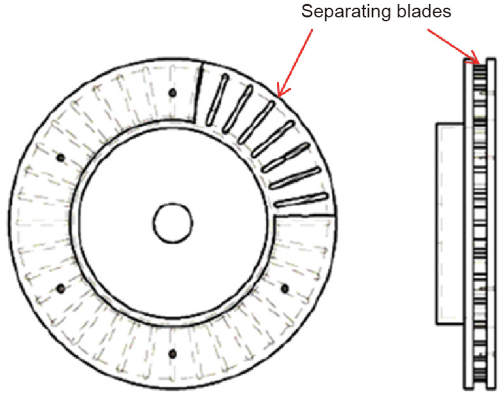

Fig. 14. General ventilated brake disk. The oblong dark shapes in the left image highlight the blades that separate the two disks of the brake in order to facilitate heat transfer to the environment through increased surface area and air flow. Reproduced from Ref. [85] with permission of Springer Nature, © 2013.

Choi and Lee [87] performed FEA on carbon–carbon disk brakes with frictional heating at the contact surfaces. They focused on the thermoelastic instability phenomenon (i.e., the unstable growth of contact pressure and temperature), and concluded that hoop stress had the greatest impact on material failure. The material's thermal expansion coefficient and elastic modulus had the greatest effect on the frictional contact surfaces. Computations were also performed with carbon–carbon composite brakes, which outperformed isotropic brakes by distributing the pressure across the entire brake pad [87]. To better simulate these conditions, however, the coefficient of friction should also be considered as a function of vehicle speed and number of wheel revolutions [88].

Tonchev et al. [88] discovered that many components throughout the underbody chassis affect accurate calculation of the brake rotor's temperature profile. To add to the contributing components, Kang et al. [89] used CFD to demonstrate that the rim spoke geometry significantly affected convective heat transfer from the rotor. These researchers simulated rims with five, six (baseline), and eight spokes, and validated their results with experimental data. The simulations consisted of a tire at a given rotational speed with air flowing past it while the rotor was set at a constant temperature. The five-spoke geometry allowed the most cooling air flow to the rotor. The same geometries were simulated with the spokes twisted at different angles (30° and 45°) to allow more cooling air flow. It was concluded that the five-spoke rim with a twist angle of 45° was the optimum rim geometry out of those tested for dissipating heat generated by friction [89].

Much of the previously discussed research has sought to dissipate heat from the rotor by better understanding and managing convection. A newer technology, known as regenerative braking, uses the frictional forces from braking to generate electrical energy that can be used elsewhere in the vehicle. Yoong et al. [90] discussed how regenerative brakes function and studied brake controllers in regenerative braking for efficiency and energy savings in an EV. For an EV or HEV vehicle, the brake controller directs the electrical charge into a battery or capacitors for recharging or storage. Some improvements to the regenerative braking system include the implementation of a flywheel and an ultracapacitor with a DC–DC converter. The flywheel system smooths variations in speed that stem from changes in torque and converts mechanical energy into electrical energy. The DC–DC converter is considered a "buck–boost" circuit, where the boost is used in acceleration and the buck in deceleration, both of which charge a capacitor. An ultracapacitor provides improved charging capacity, and the buck–boost keeps energy in the regenerative brakes to aid in acceleration while storing energy during deceleration.

4.3. Tires

An understanding of the thermal response in vehicle tires can help to predict their performance and lifetime. Tires are composed largely of rubber (Fig. 15) [91]; they deform as they come into contact with the road surface, which affects the temperature distribution in the tire as the vehicle moves. At high speeds, tires deform quickly and frequently, and the rubber's viscous and elastic behaviors cause hysteresis that generates heat. According to the Committee for the National Tire Efficiency study, which was commissioned by the National Highway Traffic Safety Administration (NHTSA) of the US Department of Transportation, hysteresis is defined as follows:

> *... a characteristic of a deformable material such that the energy of deformation is greater than the energy of recovery. The rubber compound in a tire exhibits hysteresis. As the tire*

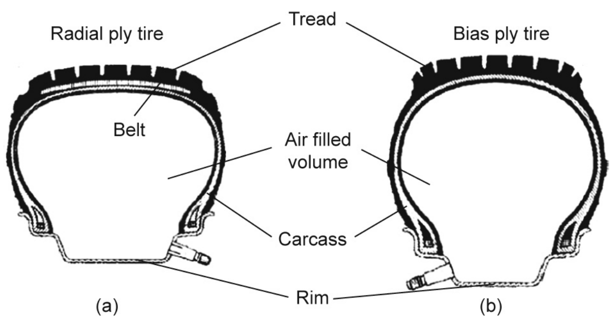

Fig. 15. A breakdown of two general tire types. (a) Radial ply tires are generally used for longer travel times because of the added durability from the steel belt; (b) bias ply tires are often cheaper and more suited for short-haul trailer applications. Reproduced from Ref. [91] with permission of Elsevier, © 2004.

rotates under the weight of the vehicle, it experiences repeated cycles of deformation and recovery, and it dissipates the hysteresis energy loss as heat. Hysteresis is the main cause of energy loss associated with rolling resistance and is attributed to the viscoelastic characteristics of the rubber [92].

With an increase in hysteretic losses, the temperature in the tire increases. Ambient conditions also affect the temperature profile of the tire and the stresses on it.

Lin and Hwang [93] modeled a smooth tread bias tire, as shown in Fig. 16. All the simulations were supported with experimental results from a light-duty truck operated at different velocities, internal pressures, and loads to predict the temperature distribution of the tire. The conclusions drawn from their study included the following: hysteresis rose in direct proportion to the load on the tire, internal pressure decreased and heat increased with rolling velocity, and internal tire pressure was key to the temperature of the tire.

Cho et al. [94] used a numerical method to predict the hysteretic losses of a periodic-patterned (treaded) tire instead of a smooth tire. With accurate prediction of tire hysteresis, rolling resistance and tire temperature could also be predicted because both are directly related to hysteretic loss. Cho et al. modeled the tire with static tire contact analysis and neglected rolling effects. Two patterned tires were modeled and compared with a simple, main-grooved tire model. The hysteresis and temperature were dependent upon the loss modulus, and the temperature was predicted by a staggered iterative method [94]. The researchers found that the highest temperature occurred at the belt edge, which was

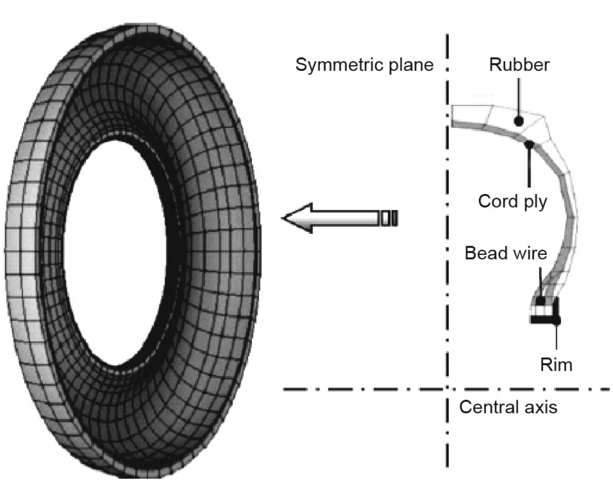

Fig. 16. Simplified finite element mesh of a bias ply tire. Reproduced from Ref. [93] with permission of Elsevier, © 2004.

similar to their experimental results, although the value predicted was less than the experimental value due to the simplification of the static tire contact analysis, which ignored the complex dynamic friction between the tire and rough surfaces. In addition, velocity affected the tire temperature, hysteresis, and rolling resistance; the heat generation increased with velocity, while hysteresis and rolling resistance decreased slightly with each increase in velocity.

Hysteresis is the main cause of increased temperature in tires, but ambient conditions also affect tire temperature. Li et al. [95] studied the effects of ambient conditions on the stress, deformation, and temperature of a modeled truck tire using FEA. A two-dimensional radial tire was simulated using a Mooney–Rivlin material model for the rubber. The simulated tire was comprised of tread, belt, carcass, and an air-filled cavity. The ambient temperature ranged from −40 to 40 °C, and the temperatures were partitioned into the winter, spring/fall, and summer seasons. From the simulations, the maximum stresses occurred in the belt region and increased as the ambient temperature increased. The tire displacement increased with temperature, and the results showed that the displacement was more affected by temperature than by the stress in the tire. These results were supported by experimental data, and the researchers concluded that an increase in ambient temperature increased the temperature in the belt and carcass regions.

4.4. Exhaust

Accurate simulation of the vehicle underbody is an important component of overall vehicle thermal management. Accurate simulations reduce reliance on costly prototypes while predicting the temperatures of sensitive underbody components. The main heat source in the undercarriage is the exhaust system [96], which is connected to the engine through different exhaust valves by way of the exhaust manifold. After the manifold, the exhaust pipe is connected to the catalytic converter and then through the muffler; finally, it is connected to the tailpipe. A general exhaust system schematic is shown in Fig. 17 [97].

To model the temperature distribution in an exhaust system, an understanding of what types of heat transfer are taking place in and around different systems is necessary [97]. For a single-wall exhaust pipe system, forced convection is present from the hot gases flowing through the pipe. Conduction through the pipe is also a factor. In addition, there is natural convection from the outside of the pipe to the surroundings when the vehicle is stationary, or forced convection when the vehicle is in motion. Non-negligible thermal radiation takes place between the outer part of the pipe and the surroundings when pipe temperatures exceed 400 °C [97]. Double-wall exhaust pipes consisting of concentric pipes are also used, with or without insulation between the two pipes. Systems with insulation may be modeled by conduction, similar to single-wall systems, while the modeling of double-wall systems with air gaps must consider an added layer of natural convection and radiation from the inner and outer walls.

Haehndel et al. [96] sought to achieve a more accurate representation of the temperature variations in two different automobile exhaust systems at 60 and 210 $km \cdot h^{-1}$. To achieve this goal, a one-dimensional fluid profile was incorporated into a three-dimensional exhaust system. Entrance, pulsation, surface, and geometry correction factors were introduced into the overall convection augmentation factor (CAF) of the simulation to solve for the complex gas flow through the curved exhaust system. The total CAF was compiled from previous literature. The two exhaust systems considered were a turbocharged spark ignition and a diesel engine with two turbochargers. Both the simulation and experimental data showed the highest temperatures within the tur-

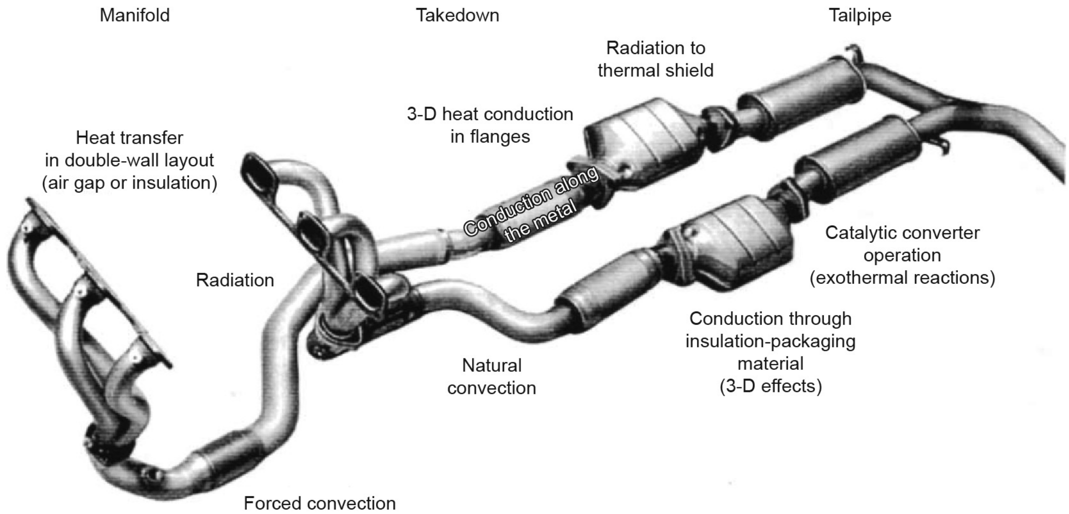

Fig. 17. Exhaust system heat transfer modes. Reproduced from Ref. [97] with permission of Professional Engineering Publishing, © 1997.

bocharger of the former (about 700 °C) and the manifold cylinder of the latter (about 425 °C).

The similarity between each different exhaust system is the manifold. The Reynolds numbers in the manifold can be below turbulent values, but this region is considered to be turbulent due to the pulsating flow. This pulsation is caused by the exhaust valves opening and closing inside the cylinder, which creates recirculation zones and causes high rates of heat transfer [97].

The manifold is exposed to the most extreme conditions, including high heat and mechanical stresses due to engine vibrations. Meda et al. [98] studied the physical design/development process for a stainless steel manifold system. The skin temperature of the manifold was simulated by means of CFD and the temperature distribution was measured experimentally. The temperature data were used as input into an FEA to calculate the thermal stresses on the manifold and locate weak points. Meda et al. altered the geometry of the manifold to strengthen it. The fatigue life of the stainless steel manifold was simulated using the Coffin–Manson law, which relates strain amplitude to fatigue life. Finally, the heat shield that covers the manifold was analyzed based on engine excitation, and high stress areas were found and corrected on the heat shield.

Major differences exist between diesel and gasoline engine exhausts. In a diesel exhaust, a turbocharger near the exit of the cylinder allows for more efficient compression of the intake air. Further down the system, a diesel particulate filter removes harmful particles, such as soot, to meet emission requirements. Laurent [99] designed a method to predict the surface temperature of a diesel exhaust system during regeneration and compared the simulations to experimental results. The method implemented a one-dimensional regeneration model and a three-dimensional CFD model for convection coefficients. The results from the analytical and CFD model were used in a three-dimensional FEA to determine the surface-temperature profile. Laurent did not consider the pressure drop in the exhaust system; therefore, backpressure effects were neglected.

4.5. Aerodynamics

The aerodynamics of a vehicle affect many aspects of its thermal management due to convective cooling. A proper investigation of aerodynamics results in a better understanding of the air flow paths and the effects on the heat generated at different points on the vehicle. If aerodynamic characteristics are understood correctly, the convective heat transfer can be more accurately modeled.

Bendell [100] conducted a thermal analysis of an entire vehicle to show the effect of temperature on its heat shields. The study considered how the simulated full-vehicle thermal problem affected the accuracy of temperature predictions. The model simulated a vehicle in a trailer-towing test as a steady-state analysis. Bendell coupled a CFD model to a thermal model, and the simulation returned useful qualitative data in the vehicle underbody, especially in areas removed from the rear of the exhaust.

Since Bendell's work in 2005, more accurate co-simulation programs have been developed and used as validation tools. With computer-aided design (CAD) models being made available early in the design process, simulated aerodynamic performance can help shape the vehicle, given that the CAD data have accurately modeled the open grill, under hood, underbody, and upper body surfaces. With a coupled simulation program, Duncan et al. [101] conducted a total vehicle analysis (TVA) that spanned multiple disciplines, such as aerodynamics, aeroacoustics, and thermal management. The drag coefficient, fan-off cooling flow rate, and static pressures were calculated from aerodynamics, wall pressure fluctuations were calculated on the upper body and under body from aeroacoustics and, finally, cooling air flow performance was computed for the entire vehicle and surface temperatures for the purposes of thermal management. The researchers took into account radiation from hot surfaces and conduction. Their extensive simulations showed that accurate CAD modeling is necessary to precisely predict a vehicle's aerodynamic, aeroacoustic, and thermal performance for use in the design process [101]. Mukutmoni et al. [102] simulated a passenger vehicle under different driving conditions, including drastic speed changes, engine idling, and unused engine cooling. The coupled flow/thermal solver took into account radiation, convection, and conduction effects, and the simulation temperatures closely matched the full-scale experimental results.

Traffic situations have also been demonstrated to have an effect on fuel consumption. In a truck platooning scenario, Narayana et al. [103] performed simulations involving two identical vehicles. Heat rejection was varied based on aerodynamic conditions induced by the leading vehicle on the trailing vehicle. The results suggested that the vehicle performance of a trailing vehicle would be reduced in a single-lane traffic scenario due to cold mass air flow velocities. This result was observed in their simulation at larger separation distances when the speed was increased.

4.6. Weather-terrain interaction

Full-vehicle thermal management requires a knowledge of how terrain and weather affect the vehicle. To experimentally determine the effects of terrain and weather, multiple days of measurements are required, as well as the ability to virtually simulate terrain and weather. The US Army Engineer Research and Development Center (ERDC) [104] created a three-dimensional test bed using an electro-optical/infrared (EO/IR) sensor, which produces a synthetic thermal image. In this test bed, terrain was modeled on an actual highland climatic zone with a rugged terrain. The researchers stated that IR images were affected by weather, time of day, soil conditions, solar load, and vegetation. In the test bed, the weather conditions could be varied, and any objects (e.g., trees, shrubs, or grass) could be inserted or removed as necessary. The test bed simulated a 5 m $\times$ 5 m region of interest with an undeveloped road running through the test site. The temperature of the region was recorded for 40 d in 5 min intervals by an onsite meteorological station. An IR camera was used to take images every 5 min for five of those days. The researchers' simulation results were similar to the collected data, despite errors introduced by sporadic cloud coverage.

Eslinger et al. [105] expanded the number of regions tested and simulated to six; this produced more conclusive data and a validation of their simulations of the highland climate zone, and demonstrated that it is possible to accurately map a region. With accurate weather and terrain simulation, a vehicle can be placed in the terrain to simulate how a specific environment might affect it.

5. Summary and future work

A wide variety of materials, devices, and systems have been invented and improved over the last few years to help enhance vehicle thermal management strategies in each of the three areas most important to the field: the cabin, power electronics, and exterior. The implementation of mature technologies and further research and development into upcoming solutions promises to yield significant benefits—not only to manufacturers and consumers, but to society as a whole.

The main challenges in the vehicle cabin are related to the HVAC system, which places a heavy demand on the vehicle prime mover (e.g., the engine or battery), thereby reducing fuel economy and range. Improvements generally focus on two areas: reducing heat absorption to lower the HVAC load, and improving the efficiency of the cooling system. Technologies such as surface glazing and tinting have been shown to reduce the heat load on a vehicle when it is exposed to the sun. However, tinted glass is permanent, and when the weather is cold, thermal soak is desirable to warm the cabin using free solar power. Photovoltachromic devices should be studied further to allow thermal soak to be varied depending on ambient conditions.

Zoned cooling technologies can decrease power demands on HVAC systems. Customers have recently found algorithmic optimization of ACC systems to be more useful than systems of the past. HVAC systems in EVs must be dealt with differently from those in conventional ICEs. Implementation of heat pumps and thermal batteries were discussed as a means to reduce the power demand from the battery pack, and further research in these areas is warranted. Heat pumps continue to be most efficient in colder climates, but have only been examined for the special case of heating electric buses, in which the heat output is greater than in smaller automobiles. More research into the performance of these devices in EVs, as well as the feasibility of operating such devices in cooling modes in hotter climates, may be warranted. Thermal batteries remain in their infancy, so studies involving their efficient integration into EVs should be pursued and efforts to improve their longevity should be made.

Some countries, such as the United States, have a very wide range of climates. Therefore, car manufacturers should focus on developing cabin thermal management systems that are appropriate for a range of environments. Future studies should comment on the system's adaptability; if a system is only suited for a particular region, it should exist as a "plug-and-play" component that can be easily incorporated into a large selection of automobiles. In general, cabin thermal management studies tend to focus on either heating or cooling the interior of a vehicle. Research into how to best implement both into a single vehicle will ultimately be necessary.

Thermal soak can be addressed via ventilation, using methods such as floor vents. However, exhaust products, dirt, and animals may enter the cabin through these vents. Thus, new methods need to be explored that provide ventilation to improve cabin temperature while avoiding unwelcome intrusions and other problems. Ventilation fans have been found to reduce thermal load effectively, but can have drawbacks similar to those of floor vents. They also have potential efficiency issues, which can be addressed through the use of solar power. On cloudy days, less power would be available, but without direct sunshine, thermal ingress should also be lower. Passenger comfort may also be increased by finding ways to control interior humidity via ventilation systems.

As electronics in vehicles become smaller, more powerful, and more important—especially in EVs—better cooling strategies become essential. The two major components of concern are the battery and the IGBT. Passive cooling of the IGBT using oscillating heat pipes has been investigated, and the results demonstrate that acetone and *n*-pentane are suitable working fluids for this application. TIMs can more efficiently transfer heat from electronic components to passive coolers. Despite the recent advances in TIMs, their cost-effective production for implementation in EV systems has not been studied in detail. Active cooling via AHSs, which transfer heat through a sealed miniature loop of liquid metal alloy, has been demonstrated to be a feasible electronics cooling solution. Another type of active cooling is jet impingement, in which heat-dissipating surfaces come in direct contact with the coolant for higher heat transfer coefficients. Methods to cool the battery pack include forced convection, heat pipes, and PCMs. Heat pipes are most effective when built into the battery wall, and can also be designed for either free or forced convection cooling. However, heat pipes have not yet been implemented in a fully operating system for an extended period of time. Research on improving heat pipe reliability may provide a more consistent, lightweight, and passive solution. Additional research on the rapid manufacturing and cost reduction of heat pipes would also prove beneficial for mass production. Improving EVs and HEVs will require finding new ways to dissipate thermal energy from the battery pack and IGBT, as well as addressing thermal design limitations.

The vehicle exterior contains many components and heat sources that affect the rest of the vehicle. The surface temperature is strongly impacted by direct sunlight, while air flow through the grill affects radiator performance and creates drag on the vehicle that reduces fuel economy. Fan sizes and shutter systems have been simulated and tested to solve the latter problem. Efforts could also be made to reduce drag by finding optimum ways of directing air flow under the hood and tire well locations. Vehicle brakes generate high heat fluxes during the braking process. Wheel spoke inclination and ventilated rotors have been found to remove and transfer the heat most effectively. Tire deformation affects tire temperature, and at high speeds, the deformations become more severe and cause high temperatures and stress on the tires. Many simulations have been carried out to study hysteresis, but the field would benefit from using this information to redesign tires that are more effective. The underbody of the vehicle is affected by heat from the exhaust system. Simulations have shown the effects of exhaust heat, but these simulations can be made more accurate by including transient temperatures associated with the hot gas flowing through the exhaust, rather than simplifying the exhaust pipe as a constant temperature heat source. Regenerative braking is a new technology in which full-scale thermal analysis is needed. Brake simulations must also consider the heat transfer in both the brake pad and the rotor. Simulations that incorporate the cyclic nature of the internal combustion engine as a heat source would be of great interest.

Acknowledgements

This effort was sponsored by the US Government under Other Transaction number W15QKN-13-9-0001 between the Consortium for Energy, Environment and Demilitarization, and the Government, with funding provided by the US Army Engineer Research & Development Center. The US Government is authorized to reproduce and distribute reprints for Governmental purposes notwithstanding any copyright notation thereon. The views and conclusions contained herein are those of the authors and should not be interpreted as necessarily representing the official policies or endorsements, either expressed or implied, of the US Government.

Compliance with ethics guidelines

Garrett J. Marshall, Colin P. Mahony, Matthew J. Rhodes, Steve R. Daniewicz, Nicholas Tsolas, and Scott M. Thompson declare that they have no conflict of interest or financial conflicts to disclose.

References

[1] Danca P, Vartires A, Dogeanu A. An overview of current methods for thermal comfort assessment in vehicle cabin. Energy Procedia 2016;85:162–9.
[2] Orofino L, Amante F, Mola S, Rostagno M, Villosio G, Piu A. An integrated approach for air conditioning and electrical system impact on vehicle fuel consumption and performances analysis: DrivEM 1.0. SAE Tech Pap 2007;116:678–86.
[3] Levinson R, Pan H, Ban-Weiss G, Rosado P, Paolini R, Akbari H. Potential benefits of solar reflective car shells: cooler cabins, fuel savings and emission reductions. Appl Energy 2011;88(12):4343–57.
[4] Rugh JP, Chaney L, Lustbader J. Reduction in vehicle temperatures and fuel use from cabin ventilation, solar-reflective paint, and a new solar-reflective glazing. SAE Tech Pap 2007: 2007-1-1194.
[5] Saidur R, Masjuki HH, Hasanuzzaman M. Performance of an improved solar car ventilator. Int J Mech Mater Eng 2009;4(1):24–34.
[6] Jha KK, Bhanot V, Ryali V. A simple model for calculating vehicle thermal loads. SAE Tech Pap 2013: 2013–01-0855.
[7] Rugh J, Farrington R. Vehicle ancillary load reduction project close-out report. An overview of the task and a compilation of the research results. Report. Washington: National Renewable Energy Laboratory; 2008 Jan. Report No.: NREL/TP-540-42454.
[8] Rugh J. Impact of Sungate EP on PHEV performance results of a simulated solar reflective glass PHEV dynamometer test. Report. Washington: National Renewable Energy Laboratory; 2009 June. Report No.: NREL/TP-540-45908.
[9] Ozeki Y, Harita Y, Hirano A, Nishihama J. Evaluation on the solar reduction glass in an electric vehicle by experimental measurements in a climate chamber. SAE Tech Pap 2014: 2014-01-0703.
[10] Jaksic NI, Salahifar C. A feasibility study of electrochromic windows in vehicles. Sol Energy Mater Sol Cells 2003;79(4):409–23.
[11] Cannavale A, Manca M, De Marco L, Grisorio R, Carallo S, Suranna GP, et al. Photovoltachromic device with a micropatterned bifunctional counter electrode. ACS Appl Mater Interfaces 2014;6(4):2415–22.
[12] Rugh JP, Farrington RB, Boettcher JA. The impact of metal-free solar reflective film on vehicle climate control. SAE Tech Pap 2001: 2001-01-1721.
[13] Lustbader JA, Venson T, Adelman S, Dehart C, Yeakel S, Castillo MS. Application of sleeper cab thermal management technologies to reduce idle climate control loads in long-haul trucks. SAE Tech Pap 2012: 2012-01-2052.
[14] Wolfe N, Mu X, Huang L, Kadle P. Cooling with augmented heated and cooled seats. SAE Tech Pap 2007: 2007-01-1193.
[15] Wang M, Wolfe E, Ghosh D, Bozeman J, Chen K, Han T, et al. Localized cooling for human comfort. SAE Tech Pap 2014: 2014-01-0686.
[16] Ghosh D, Wang M, Wolfe E, Chen K, Kaushik S, Han T. Energy efficient HVAC system with spot cooling in an automobile—design and CFD analysis. SAE Tech Pap 2012:2012-01-0641.
[17] Kaushik S, Chen K, Han T, Khalighi B. Micro-cooling/heating strategy for energy efficient HVAC system. SAE Int J Mater Manuf 2011;4(1):853–63.
[18] Wang M, Ghosh D, Wolfe E, Chen K, Bozeman J. Energy efficiency impact of localized cooling. SAE Tech Pap 2014: 2014-01-0695.
[19] Salaün F, Devaux E, Bourbigot S, Rumeau P. Development of phase change materials in clothing part I: formulation of microencapsulated phase change. Text Res J 2010;80(3):195–205.
[20] Matheson R. 'Cool' invention wins first place at MADMEC [Internet]. Cambridge: MIT News Office; 2013 [cited 2017 Jun 15]. Available from: http://newsoffice.mit.edu/2013/madmec-design-competition-1017#.Ul_1KuUbJy0.
[21] Kolbe WH, Yott EW, Brown BB, Gaskill GM, Martin W. The 1964 cadillac comfort control. SAE Tech Pap 1964: 640829.
[22] Wang M, Pawlak JL, Archibald CA. Development of next generation automatic climate control. SAE Tech Pap 2007: 2007-01-1188..
[23] Fayazbakhsh MA, Bahrami M. Comprehensive modeling of vehicle air conditioning loads using heat balance method. SAE tech Pap 2013: 2013-01-1507.
[24] Marcos D, Pino FJ, Bordons C, Guerra JJ. The development and validation of a thermal model for the cabin of a vehicle. Appl Therm Eng 2014;66(1–2):646–56.
[25] Donovan P, Manning J. Strategy for efficient automotive climate control. SAE Tech Pap 2007: 2007-01-1190..
[26] Song S, Cai W, Wang YG. Auto-tuning of cascade control systems. ISA Trans 2003;42(1):63–72.
[27] Zaheer-uddin M, Tudoroiu N. Neuro-PID tracking control of a discharge air temperature system. Energy Convers Manage 2004;45(15–16):2405–15.
[28] Khayyam H, Kouzani AZ, Hu EJ, Nahavandi S. Coordinated energy management of vehicle air conditioning system. Appl Therm Eng 2011;31(5):750–64.
[29] Furse D, Park S, Foster L, Real Kim S. world customer usage of the Hyundai Genesis climate control system in the USA. SAE Tech Pap 2014: 2014-01-0685.
[30] Kilic M, Akyol SM. Experimental investigation of thermal comfort and air quality in an automobile cabin during the cooling period. Heat Mass Transf 2012;48(8):1375–84.
[31] Mathur GD. Experimental investigation to monitor tailpipe emissions entering into vehicle cabin to improve indoor air quality (IAQ). SAE Tech Pap 2007: 2007-01-0539.
[32] Grady ML, Jung H, Kim YC, Park JK, Lee BC. Vehicle cabin air quality with fractional air recirculation. SAE Tech Pap 2013: 2013-01-1494.
[33] Farrington R, Rugh J. Impact of vehicle air-conditioning on fuel economy, tailpipe emissions, and electric vehicle range. In: Proceedings of the Earth Technologies Forum; 2000 Oct 31; Washington, DC, USA. Golden: National Renewable Energy Laboratory; 2000.
[34] Kambly KR, Bradley TH. Estimating the HVAC energy consumption of plug-in electric vehicles. J Power Sources 2014;259:117–24.
[35] Torregrosa-Jaime B, Payá J, Corberan J. Design of efficient air-conditioning systems for electric vehicles. SAE Tech Pap 2013: 2013-01-0864.
[36] Cho CW, Lee HS, Won JP, Lee MY. Measurement and evaluation of heating performance of heat pump systems using wasted heat from electric devices for an electric bus. Energies 2012;5(3):658–69.
[37] Taylor R, Chung CY, Morrison K, Hawkes ER. Analysis and testing of a portable thermal battery. J Therm Sci Eng Appl 2014;6(3):031004.
[38] Velivelli A, Guerithault D, Stowe S. Optimum seat cooling distribution for targeted human thermal comfort. SAE Int J Passeng Cars Mech Syst 2017;10(1):128–34.
[39] Attar A, Lee H. Designing and testing the optimum design of automotive air-to-air thermoelectric air conditioner (TEAC) system. Energy Convers Manage 2016;112:328–36.
[40] Wang D, Crane D, LaGrandeur J. Design and analysis of a thermoelectric HVAC system for passenger vehicles. SAE Tech Pap 2010: 2010-01-0807.
[41] Ito Y, Sakoi T, Miyamoto T. Evaluation method of thermal sensation and comfort for air conditioning performance reduction. SAE Tech Pap 2018: 2018-01-0775.
[42] Nielsen F, Uddheim Å, Dalenbäck JO. Potential energy consumption reduction of automotive climate control systems. Appl Therm Eng 2016;106:381–9.
[43] Vlahinos A, Pesaran AA. Energy efficient battery heating in cold climates. SAE Tech Pap 2002: 2002-01-1975.
[44] Grover GM, Cotter TP, Erickson GF. Structures of very high thermal conductance. J Appl Phys 1964;35(6):1990–1.
[45] Peterson GP. An introduction to heat pipes: modeling, testing and application. New York: John Wiley & Sons; 1994.
[46] Zhang Y, Faghri A. Advances and unsolved issues in pulsating heat pipes. Heat Transf Eng 2008;29(1):20–44.
[47] Burban G, Ayel V, Alexandre A, Lagonotte P, Bertin Y, Romestant C. Experimental investigation of a pulsating heat pipe for hybrid vehicle applications. Appl Therm Eng 2013;50(1):94–103.
[48] Connors MJ, Zunner JA. The use of vapor chambers and heat pipes for cooling military embedded electronic devices. In: Proceedings of the 2009 IEEE Military Communications Conference; 2008 Aug 10–14; Jacksonville, FL, USA. New York: IEEE; 2009.
[49] Tang X, Park C. Vibration/shock-tolerant capillary two-phase loop technology for vehicle thermal control. In: Proceedings of the 2008 ASME Summer Heat

Transfer Conference; 2008 Aug 10–14; Jacksonville, FL, USA. New York: American Society of Mechanical Engineers; 2008. p. 1–7.
[50] Otiaba KC, Ekere NN, Bhatti RS, Mallik S, Alam MO, Amalu EH. Thermal interface materials for automotive electronic control unit: trends, technology and R&D challenges. Microelectron Reliab 2011;51(12):2031–43.
[51] Kelly KJ, Abraham T, Bennion K, Bharathan D, Narumanchi S, Keefe MO. Assessment of thermal control technologies for cooling electric vehicle power electronics. Report. Washington: National Renewable Energy Laboratory; 2008 Jan. Report No.: NREL/TP-540-42267.
[52] Tang B, Hu G, Gao H, Hai L. Application of graphene as filler to improve thermal transport property of epoxy resin for thermal interface materials. Int J Heat Mass Transfer 2015;85:420–9.
[53] Zeng L, Liu Y, Chang W, Zhang L, Ding Z, Wang W, et al., inventors; Honeywell international Inc., assignee. Compressible thermal interface materials. United States patent US 10068830 B2. 2018 Sep 4.
[54] Chen J, Huang X, Sun B, Wang Y, Zhu Y, Jiang P. Vertically aligned and interconnected boron nitride nanosheets for advanced flexible nanocomposite thermal interface materials. ACS Appl Mater Interfaces 2017;9(36):30909–17.
[55] Chang TC, Liao CA, Lin ZY, Fuh YK. Highly stretchable thermal interface materials with uniformly dispersed network of exfoliated graphite nanoplatelets via ball milled processing route. Microsyst Technol 2018;24(9):3667–75.
[56] Vetrovec J. High-performance heat sink for interfacing hybrid electric vehicles inverters to engine coolant loop. SAE Tech Pap 2011: 2011-01-0349.
[57] Woo BG, Lee Y, Kang CH, Cho KY. Water cooling radiation method for inverter system of hybrid electric vehicles. In: Proceedings of the 31st International Telecommunications Energy Conference; 2009 Oct 18–22; Incheon, Korea. New York: IEEE; 2009.
[58] Mudawar I, Bharathan D, Kelly K, Narumanchi S. Two-phase spray cooling of hybrid vehicle electronics. IEEE Trans Compon Packag Tech 2009;32(2):501–12.
[59] Bostanci H, Van Ee D, Saarloos BA, Rini DP, CHow LC. Thermal management of power inverter modules at high fluxes via two-phase spray cooling. IEEE Trans Compon Packag Manuf Technol 2012;2(9):1480–5.
[60] Narumanchi S, Troshko A, Bharathan D, Hassani V. Numerical simulations of nucleate boiling in impinging jets: applications in power electronics cooling. Int J Heat Mass Transfer 2008;51(1–2):1–12.
[61] Narumanchi S, Kelly K, Mihalic M, Gopalan S, Hester R, Vlahinos A. Single-phase self-oscillating jets for enhanced heat transfer. In: Proceedings of the 2008 24th Annual IEEE Semionductor Thermal Measurement Management Symposium; 2008 Mar 16–20; San Jose, CA, USA. New York: IEEE; 2008. p. 154–62.
[62] Panchal S, Dincer I, Agelin-Chaab M, Fraser R, Fowler M. Thermal modeling and validation of temperature distributions in a prismatic lithium-ion battery at different discharge rates and varying boundary conditions. Appl Therm Eng 2016;96:190–9.
[63] Rao Z, Wang S. A review of power battery thermal energy management. Renew Sustain Energy Rev 2011;15(9):4554–71.
[64] Wang Q, Jiang B, Li B, Yan Y. A critical review of thermal management models and solutions of lithium-ion batteries for the development of pure electric vehicles. Renew Sustain Energy Rev 2016;64:106–28.
[65] Swanepoel G. Thermal management of hybrid electrical vehicles [dissertation]. Stellenbosch: University of Stellenbosch; 2001.
[66] Rao Z, Wang S, Wu M, Lin Z, Li F. Experimental investigation on thermal management of electric vehicle battery with heat pipe. Energy Convers Manage 2013;65:92–7.
[67] Rao Z, Huo Y, Liu X. Experimental study of an OHP-cooled thermal management system for electric vehicle power battery. Exp Therm Fluid Sci 2014;57:20–6.
[68] Greco A, Cao D, Jiang X, Yang H. A theoretical and computational study of lithium-ion battery thermal management for electric vehicles using heat pipes. J Power Sources 2014;257:344–55.
[69] Tran TH, Harmand S, Desmet B, Filangi S. Experimental investigation on the feasibility of heat pipe cooling for HEV/EV lithium-ion battery. Appl Therm Eng 2014;63(2):551–8.
[70] Tran TH, Harmand S, Sahut B. Experimental investigation on heat pipe cooling for hybrid electric vehicle and electric vehicle lithium-ion battery. J Power Sources 2014;265:262–72.
[71] Zou H, Wang W, Zhang G, Qin F, Tian C, Yan Y. Experimental investigation on an integrated thermal management system with heat pipe heat exchanger for electric vehicle. Energy Convers Manage 2016;118:88–95.
[72] Ling Z, Zhang Z, Shi G, Fang X, Wang L, Gao X, et al. Review on thermal management systems using phase change materials for electronic components, Li-ion batteries and photovoltaic modules. Renew Sustain Energy Rev 2014;31:427–38.
[73] Ling Z, Chen J, Fang X, Zhang Z, Xu T, Gao X, et al. Experimental and numerical investigation of the application of phase change materials in a simulative power batteries thermal management system. Appl Energy 2014;121:104–13.
[74] Xu B, Leffert M, Belanger B. Fuel economy impact of grille opening and engine cooling fan power on a mid-size sedan. SAE Tech Pap 2013: 2013-01-0857..
[75] Jama H, Watkins S, Dixon C. Reduced drag and adequate cooling for passenger vehicles using variable area front air intakes. SAE Tech Pap 2006: 2006-01-0342.
[76] Charnesky S, Fadler G, Lockwood T. Variable and fixed airflow for vehicle cooling. SAE Int J Mater Manuf 2011;4(1):1286–96.
[77] Pfeifer C. Evolution of active grille shutters. SAE Tech Pap 2014: 2014-01-0633.
[78] Bonkoski P, Karnik AY, Fuxman A. Calibration and demonstration of vehicle powertrain thermal management using model predictive control. SAE Int J Engines 2017;10(2):173–80.
[79] Kubokura T, Uno T, Evans N, Kuroda H, Shindo F, Nagahama S. Study of cooling drag reduction method by controlling cooling flow. SAE Tech Pap 2014: 2014-01-0679.
[80] Baeder D, Indinger T, Adams N, Unterlechner P. Aerodynamic investigation of vehicle cooling drag. SAE Tech Pap 2012: 2012-01-0170.
[81] Kuthada T, Wiedemann T. Investigations in a cooling air flow system under the influence of road simulation. SAE Tech Pap 2008: 2008-01-0796.
[82] Belhocine A, Mostefa B. Thermomechanical stress analysis of vehicles gray cast brake. SAE Tech Pap 2013: 2013-01-9116.
[83] Gao CH, Lin XZ. Transient temperature field analysis of a brake in a non-axisymmetric three-dimensional model. J Mater Process Technol 2002;129:513–7.
[84] Timur M, Kuscu H. Heat transfer of brake pad used in the autos after friction and examination of thermal tension analysis. Mechanics 2014;20(1):17–23.
[85] Munisamy KM, Shuaib NH, Yusoff MZ, Thangaraju SK. Heat transfer enhancement on ventilated brake disk with blade inclination angle variation. Int J Automot Technol 2013;14(4):569–77.
[86] Munisamy KM, Shafik R. Disk brake design for cooling improvement using computational fluid dynamics (CFD). IOP Conf Ser: Earth Environ Sci 2013;16:012109.
[87] Choi J, Lee I. Finite element analysis of transient thermoelastic behaviors in disk brakes. Wear 2003;257(1–2):47–58.
[88] Tonchev A, Hirschberg W, Jagsch S. Investigation of the thermal vehicle brake behavior during the vehicle's development phase by co-simulation. SAE Tech Pap 2007: 2007-01-3935..
[89] Kang N, Zheng W, Liu X. An investigation of the influence of the wheel spoke type on the convective cooling of the brake disc using the CFD method. Proc Inst Mech Eng, D J Automob Eng 2013;227(11):1578–89.
[90] Yoong MK, Gan YH, Gan GD, Leong CK, Phuan ZY, Cheah BK, et al. Studies of regenerative braking in electric vehicle. In: Proceedings of the 2010 IEEE Conference on Sustainable Utilization and Development in Engineering and Technology; 2010 Nov 20–21; Petalling Jaya, Malasia. New York: IEEE; 2010. p. 40–5.
[91] Fervers CW. Improved FEM simulation model for tire–soil interaction. J Terramechs 2004;41(2–3):87–100.
[92] National Research Council of the National Academies. Tires and passenger vehicle fuel economy; informing consumers, improving performance. Washington: Transportation Research Board; 2006.
[93] Lin YJ, Hwang SJ. Temperature prediction of rolling tires by computer simulation. Math Comput Simul 2004;67(3):235–49.
[94] Cho JR, Lee HW, Jeong WB, Jeong KM, Kim KW. Numerical estimation of rolling resistance and temperature distribution of 3-D periodic patterned tire. Int J Solids Struct 2013;50(1):86–96.
[95] Li Y, Liu WY, Frimpong S. Effect of ambient temperature on stress, deformation and temperature of dump truck tire. Eng Fail Anal 2012;23:55–62.
[96] Haehndel K, Frank T, Christel FM, Spengler C. Suck G, Abanteriba S, The development of exhaust surface temperature models for 3D CFD vehicle thermal management simulations part 1—general exhaust configurations. SAE Tech Pap 2013: 2013-01-0879.
[97] Konstantinidis PA, Koltsakis GC, Stamatelos AM. Transient heat transfer modelling in automotive exhaust systems. Proc Inst Mech Eng Part C 1997;211(1):1–15.
[98] Meda L, Shu Y, Romzek M. Exhaust system manifold development. SAE Tech Pap 2012: 2012-01-0643.
[99] Laurent JCM. Transient thermal simulation process over a diesel exhaust system during regeneration. SAE Tech Pap 2011: 2011-01-0658.
[100] Bendell E. Investigation of a coupled CFD and thermal modelling methodology for prediction of vehicle underbody temperatures. SAE Tech Pap 2005: 2005-0-2044.
[101] Duncan BD, Senthooran S, Hendriana D, Sivakumar P, Freed D, Gleason M, et al. Multi-disciplinary aerodynamics analysis for vehicles: application of external flow simulations to aerodynamics, aeroacoustics and thermal management of a pickup truck. SAE Tech Pap 2007: 2007-01-0100.
[102] Mukutmoni D, Alajbegovic A, Han J. Numerical simulation of transient thermal convection of a full vehicle. SAE Tech Pap 2011: 2011-01-0645.
[103] Narayana S, Vegendla P, Sofu T, Saha R, Hwang LK, Kumar MM. Investigation on underhood thermal analysis of truck platooning. SAE Int J Commer Veh 2018;11(1):5–16.
[104] Eslinger OJ, Winton C, Hines AM, Goodson R, Howington SE, Kala R. Examining the sensitivity of simulated surface temperatures due to meteorological conditions. In: Broach JT, Holloway JH, editors. Detection and sensing of mines, explosive objects, and obscured targets XVII. Bellingham: SPIE; 2012.
[105] Eslinger OJ, Hines A, Winton C, Howington SE, Fairley J, Kala R, et al. GEOTACS: countermine computational testbed results for an undifferentiated highlands climatic zone, part 1. Vicksburg: US Army Engineering Research and Development Center; 2012. Report No.: ERDC TR-12-13.